FLIGHT FLUTTER TESTING TECHNOLOGY AT GRUMMAN

H. J. Perangelo
Grumman Data Systems Corporation

F. W. Milordi
Grumman Aerospace Corporation

13

SUMMARY

The stringent requirements for flutter testing modern-day aircraft have led Grumman to develop new analysis techniques to be used in its Automated Telemetry Station for on-line data reduction. The initial technique developed by Grumman utilized a least-squares difference-equation linear-systems identification approach to extract resonant frequency and damping coefficient information from digitally filtered input and response data. This technique was successfully used on the F-14A flutter program starting in 1971, providing a quantum increase in capability relative to previously used techniques. The main advantages of the approach are

(1) Multimodal (highly coupled) analysis capability
(2) Quantitive answers for highly damped modes
(3) Ability to handle fast shaker sweeps (2 to 70 Hz in 15 sec)

These advantages, coupled with the computational and data storage capacity of the ATS, reduced test time, saved fuel, and significantly increased flight test efficiency.

Grumman has since expanded its flutter data reduction capability to encompass correlation, random decrement, and spectral techniques which are used in conjunction with its least-squares difference-equation identification approach to determine modal characteristics of response signals excited either by deterministic or random means. Cross-correlation data preconditioning techniques have exhibited superior noise rejection characteristics relative to the digital filtering approach initially employed; however, the proper utilization of these techniques generally requires an increase in data record length or sweep time. This is particularly evident when response signals are of a bimodal nature or contain low frequency modes (<10 Hz). Autocorrrelation functions and random decrement signatures analyzed via the Grumman identification approach show similar trends. From the standpoint of computational time, the random decrement method is preferred over the autocorrelation approach for the analysis of randomly excited data, while from an accuracy viewpoint both methods are equivalent.

The analysis of a nonlinear resonant system via a simplified least-squares response-error modeling technique has been successfully demonstrated.

Grumman is currently evaluating the feasibility of employing more complex versions of this identification approach to expand its flight flutter testing capability.

INTRODUCTION

Since 1970, significant strides have been made in reducing flight test flutter response data. These strides have resulted from the marriage of modern digital computing capability with new analysis techniques. Grumman's contribution has been made through the effective application of its least-squares difference-equation (LSDE) identification approach. The successful utilization of this analysis technique required an on-line interactive computer system. This system was embodied in the Grumman Automated Telemetry Station (ATS) which played an instrumental role in the timely completion of the F-14A flutter program. Staying abreast of the rapidly changing technology in the area of flight flutter testing has resulted in the development of a broad range of software programs encompassing many of the latest techniques. The value of these new data processing techniques is enhanced when used in conjunction with the LSDE identification approach. The section "Analysis Software Description" outlines how these new techniques have been implemented in application programs for use in the ATS. Appendix A contains a detailed mathematical description of the concepts that form the basis for the software algorithms used (all equation references in the body of this paper refer to relationships defined in the appendixes).

The section "Software Interactive Capabilities" describes the control the user has in interfacing with the various on-line analysis programs. Both system and program options are discussed, with emphasis placed on the program options that directly influence the quality of results. Verification of the software's technical base is discussed in the section "Test Results From Simulated Data." An analog computer six-degrees-of-freedom structural model, containing closely coupled modes, was used to generate response data with known modal characteristics. These data provided an absolute reference for evaluating software accuracy. The various programs were used to assess the modal characteristics of signals from clean sweeps, noisy sweeps, and randomly excited response data. Numerous runs were statistically analyzed to give an indication of the consistency of these programs.

Analysis of flight data with the various programs is discussed in the section "Test Results From Flight Data." The data analyzed included unimodal and bimodal response signals excited via a swept frequency shaker and/or random aerodynamic forces. The frequencies of the various modes analyzed ranged from 5.0 to 60.0 Hz with damping coefficients ranging from 0.075 to 0.25.

A nonlinear response-error modeling analysis approach, currently under investigation by Grumman, is described in the section "Current Developmental Activity." Some preliminary results obtained in the analysis of a hard-spring nonlinear resonant system are also discussed. A mathematical description of the approach used is contained in Appendix B.

BACKGROUND

Prior to 1970 the flight flutter testing methods relied primarily upon manual and analog analysis techniques such as log decrement, vector plotting, and reciprocal amplitude for structural stability indications. These methods were adequate for the classical analysis of clean signals which contained modes that were relatively uncoupled. However, an aircraft's structural response does not always approach this classical mold, and such phenomena as buffet, multimodal response, high damping, and nonlinearities severely limit the accuracy of these techniques. This resulted in a minimum of reliable and quantified answers being obtained during a test program, putting great pressure on the flutter test team and making experience and intuition rather than concrete information the prime decision maker. At times, luck was not a small part of success. Inherent in this situation was a well-founded concern for safety of flight, which resulted in the use of small test increments and numerous test altitudes. The cost of a flutter program was high in terms of number of flights and length of calendar time. The trend toward more sophisticated aircraft attaining high Mach numbers and dynamic pressures, coupled with the change in design requirement toward more flexible light weight structures, minimized predicted flutter margins and put additional pressures on the flutter test team. It became obvious that experience and intuition were not enough, the need was for better quantitative data which demanded new analytical test tools.

In this time frame, an overall change in test requirements and philosophy were sparked by time constraints set on the Grumman F-14A test program. Not only did flight flutter testing have to be expedited but so did all other discipline testing. Maximum results in the shortest calendar time was the requirement; the solution was the application of a high-speed digital computer system, new analysis techniques, telemetry of data, multidiscipline testing, and inflight refueling. Digital computers would provide speedy calculation of results, telemetry and multidiscipline testing would maximize the answers obtained at a given test point, and inflight refueling would increase flight duration. The computer system would be on-line to accept user inputs to update analysis parameters during the actual test sequence or in intermaneuver processing conducted during refueling. The objective was to reduce the traditional day-to-day data turnaround time to that of the refueling duration while achieving a simultaneous improvement in accuracy and confidence. This concept of an interactive on-line computer system become a reality in 1968 when Grumman made a large capital investment to purchase hardware and to develop system and application software to satisfy flight test requirements. The hardware/software system developed is called the Automated Telemetry Station.

AUTOMATED TELEMETRY STATION

The ATS consists of 3 major hardware subsystems. These are the Telemetry Formatter, Preprocessor, and Central Computer/Display Subsystems. A short description of each now follows:

The Telemetry Formatter subsystem receives the transmission from the aircraft, simultaneously recording and decoding the data stream for transfer to the Preprocessor. Additional functions such as time-code translation/generation, filtering, and output to analog display devices are also accomplished here.

The Preprocessor subsystem accepts the data from the Telemetry Formatter and performs the following tasks:

(1) Syllabizes bit streams into appropriate word lengths
(2) Maintains synchronization between the bit streams and the Formatter
(3) Converts data to engineering units via fifth-order calibration polynomials and limit checks it
(4) Records converted data on magnetic tape in central computer compatible format (optional)
(5) Buffers data into 0.1 second blocks and transfers the blocks on demand to the central computer at a maximum word rate of 15 000 per second
(6) Controls and monitors the Telemetry Formatter for the central computer

The Central Computer/Display Subsystem initiates operation of the ATS, performs analysis of selected data received from the Preprocessor and responds to user requests from the Data Analysis Station (DAS), an interactive console and graphic display device. The central computer can display data or calculated answers to the analyst at the remote DAS display. From this location, the analyst can request the central computer to configure the ATS, initialize real-time programs, change analysis parameters through interactive displays, process real-time data and display results, display test data on the display console screen or brush recorders, and record console displays (containing answers, data, or parametric information) on either hardcopy or microfilm.

Data flow management (figure 1) begins when the telemetry signal, containing frequency modulated (FM) and pulse-code modulated (PCM) components, is transmitted from the test aircraft. The data are received by a remote tracking antenna and relayed via a microwave link to the ATS. Data flows to a radio-frequency (RF) section which demodulates the data stream into 3 tracks, one carrying 26 500 words per second of PCM data and two carrying 14 channels each of FM flutter response data on proportional bandwidth subcarriers. The demodulated FM information then flows to the Analog to Digital Converter (ADC) which samples each parameter at 500 samples per second.

The data from the ADC is then transferred to the preprocessor. The serial PCM data flows to the Bit Synchronizer, which shapes the PCM pulse(s) and transfers them to the preprocessor for conversion to parallel format. The preprocessor collects, converts, and blocks the data for shipment to the central computer. Data transferred to the central computer is directly passed to the disk memory unit, a portion of which is allocated to the storage of 9 million words (i.e., 10 minutes of data at Grumman's normal flutter

test data rate of 15 000 words per second - which is ample capacity for thirty 15-second shaker sweeps). Data flows from the disk to the central processor unit (CPU) where it is analyzed by the specified program. Results in the form of plots and tabulations are displayed on the cathode ray tube (CRT) of the DAS. Copies of these displays are produced by the hardcopy and/or microfilm units. In parallel with the digital data flow, the outputs of the FM discriminators are displayed on Brush Tables in proximity to the DAS console.

FLUTTER TEST PHILOSOPHY

Every aircraft manufacturer performs flutter testing in order to verify predicted aeroelastic characteristics and comply with customer specifications. Paramount in the flight flutter test program is the assurance of crew safety while quantitatively identifying the structural stability of an expensive prototype aircraft.

Flight flutter testing would be trivial if flutter analyses were able to conclusively predict all flutter mechanisms, modal frequency and damping trends, and flutter speeds. Realistically, the flutter analyses are used as a baseline guide by the flutter test team as indicators of critical mechanisms and associated flutter speeds. Although predictions that agree with test results increase everyone's confidence, the decision for envelope expansion must be based on actual data and the answers derived from that data.

The potential destructive nature of flutter demands a cautious, systematic buildup in both airspeed and Mach number initiated at subcritical speeds. Aircraft structural responses are carefully monitored during accelerations to the planned test points. Data acquired at each point are completely analyzed, plotted, and extrapolated to the next test point prior to continued envelope expansion. The planned test points are continually altered based on the existing trends - too steep a trend will decrease test increments whereas a shallow trend will increase the increment. Inherent in this situation is the assumption that accurate, quantitative answers are being acquired from the analysis techniques. The objective during flight flutter testing is to acquire the best available decision base. Every effort is made to supply high quality response and driving function data to the analysis software. For example, if data acquired during a shaker sweep are noisy due to buffet response, the sweep will be repeated at a higher shaker gain setting in order to increase the signal-to-noise ratio. However, there will be times when increasing the shaker gain will not significantly improve the signal-to-noise ratio; then, techniques which precondition the data via correlation methods will be utilized to improve answer accuracy. These superior noise rejection techniques generally require a larger data sample and increased analysis time, but this may be necessary to insure accurate and consistent results.

The Grumman flutter flight test engineer has several different software programs, containing various analysis techniques, to choose from. Depending on the type of test program, one or more of these analysis programs will be utilized. They range from the TLEFAD program, which is used when information relative to the aircraft modal frequencies at the given test condition are

known, to the RESIDO program, which assumes that frequency information is not known and first calculates a frequency response function. Provisions for analyzing clean and noisy swept frequency responses, transients, and purely random excitation are contained within these programs. The ability to select different analysis techniques gives the flight test team complete flexibility to handle the flutter testing of a new aircraft design, the modification of an existing aircraft, or a nonscheduled evaluation requiring quick response. In all cases, the emphasis is on the best answers with minimum test costs.

ANALYSIS SOFTWARE DESCRIPTION

Software Overview

The ATS provides the test analyst with a powerful and flexible means of performing the on-line analysis of test data. This facility allows individual, FORTRAN coded, application programs with specific analysis capabilities to be quickly called upon to analyze or re-analyze telemetered test data as the need arises. Grumman has developed a number of different application programs, to be used in the ATS, for the purpose of reducing flutter response data to determine its modal characteristics.

The application programs were designed to provide sufficient analytical flexibility to handle adequately all expected test requirements. As such, the analytical methods employed had to be capable of analyzing flutter response data with or without a measured driving function signal and are compatible with any one of the following means of structural excitation:

(1) Swept frequency excitation
(2) Random excitation
(3) Abrupt control surface inputs
(4) Shake and stop excitation
(5) Impulsive input excitation

The LSDE identification algorithm provides the primary means of extracting resonant frequency and damping coefficient information. This identification technique is capable of handling complex multimodal response signals and is well suited to the analysis of data containing those highly coupled modes encountered as the flutter speed is approached.

The dominant assumption underlying this identification approach is that the response data is generated by a linear dynamic system. Initially, the technique was applied to the analysis of digitally filtered swept frequency test data in support of the F-14A flutter program. (See references 1 and 2.) The linearity assumption allows the identification approach to also be applied to signals that have been preprocessed by the following methods:

(1) Cross-correlation of system input and response with another function
(2) Autocorrelation of system response when system excitation is random or has a broadband-flat spectrum

(3) Random decrement signature of system response when excitation is random

The mathematical theory underlying the utilization of the above methods, in conjunction with the LSDE identification algorithm, to analytically determine system resonant frequency and damping coefficient information is explained in Appendix A.

Grumman currently has, at its disposal, three primary and two supporting applications programs to assist in reducing flutter response data at its ATS facility. The primary programs all use the LSDE identification algorithm, in conjunction with one or more of the previously mentioned data preprocessing techniques, to extract modal information. Program selection is predicated on the user's knowledge of the response data being analyzed rather than the analytical methods to be used.

If knowledge about the modal content of the test signals is available, data reduction is usually accomplished through the utilization of the TLEFAD program. Conversely, if little is known about the data or if it is desired to obtain an overall view of the modal content, either the RESIDO or ENERGY programs would be used. These programs determine the modal characteristics of the data from calculated frequency response functions. The COQUAD and APSD programs also compute frequency domain information that is sometimes helpful in establishing the modal content of response data. These latter two programs do not use the LSDE identification approach to establish modal characteristics and are normally used only in a supporting role. A utilization-oriented description of these five applications programs is given in the following discussion.

Tracking Known Modes

The TLEFAD analysis program was specifically designed to track the migration of modal resonant frequencies and damping coefficients as the flight envelope of an aircraft is expanded. The application of this program requires that the user have some knowledge of the modal composition of the flutter response data, this information being provided from previous engineering flutter analysis, ground vibration surveys, earlier test results, etc. The ability of the TLEFAD program to handle rapid shaker sweeps, simultaneously analyzing data from a number of different response transducers (up to 14 per sweep), allows this program to be particularly productive. This program plays an important role whenever timely decisions on aircraft flight test envelope expansion must be made since inherent speed of computation, flexibility, and noise rejection are improved by use of known modal information. In addition, cross checking by analysis of data from independent response transducers enhances user confidence in the resonant frequency and damping results obtained.

TLEFAD estimates modal characteristics via the LSDE identification approach. Analysis options in the program allow the user to select the preprocessing method to be used in the reduction of various types of response

data. For example, if the test data consisted of forced system response and input signals embedded in a moderate amount of noise, the data could simply be digitally band-pass filtered to highlight the mode or modes of interest in each frequency range. This filtered data would then be used in conjunction with the difference-equation model defined by equation (25) to determine resonant frequency and damping coefficient information. If, on the other hand, similar type data were to be analyzed in a highly noisy environment, increased noise rejection could be obtained by selecting the cross-correlation analysis preprocessing option. Here the driving function signal (or some function related to it such as a shaker tuning signal) would be digitally band-pass filtered over the frequency range of interest, and cross-correlated with the unfiltered response and driving function signals. The resulting cross-correlation functions would then be used in the difference-equation model defined by equation (26) for parameter identification purposes.

If the test data represents response signals driven by random excitation or by an input signal whose spectrum is broadband-flat, the response data can be preprocessed by autocorrelation methods. A calculated autocorrelation function can be used in conjunction with equation (27) to establish modal frequency and damping results. However, the difference-equation model defined by equation (28) is actually used when the autocorrelation preprocessing option is selected. This equation uses the cross-correlation function between digitally band-pass filtered response and unfiltered response signals, instead of the true autocorrelation function, and yields better results because it emphasizes the modal response in the frequency range of interest.

From this discussion, it is evident that in order to effectively use the TLEFAD program the user should have some approximate knowledge of the significant modal frequencies expected in the test data. This information provides the basis for specifying difference-equation model order, as defined by the constant N in equation (24), and for establishing the pass-band to be used in the digital filtering of the raw test data. In addition, the user selects the segment of data to be analyzed by either specifying an elapsed time duration or a frequency range in the case of swept frequency excitation. In this latter case, the program computes the instantaneous frequency of the shaker signal and processes data, for the indicated transducers, over the specified frequency range of interest using the selected preprocessing option and difference equation model order. Generally, the critical item is the selection of the filter pass-band and not the analysis data segment which can have a wide frequency range.

The primary output of the program consists of a tabulation of the resonant frequency and damping coefficient results obtained for each specified mode in every data segment. These results are augmented by diagnostic information (denoted by numerical flags such as -1.0 or -1.5 in the damping coefficient column) if the real poles are detected or if difficulties are encounted in extracting all the roots of the specified difference-equation model. Auxiliary information defining aircraft altitude, airspeed, and Mach number are also included in this tabular CRT output. Secondary CRT outputs of the program include a tabulation of backup (validation) data used in assessing the accuracy of results, a plot of calculated shaker frequency versus time

when swept frequency data are analyzed, and plots of any computed correlation functions. Examples of typical program outputs, in response to the cross-correlation analysis of the noisy swept frequency response data shown in figure 2, are set forth in figures 3 to 7.

Identifying Unknown Modes

Several different on-line programs are used to aid in the determination of the modal composition of flutter response data. These programs vary in the complexity of their analytical manipulations but are similar in that they all provide frequency domain information that forms the basis for ascertaining the modal content of the data. For example, the APSD program is often called upon to provide a power spectral density plot of a given response signal. The primary purpose of this program is to provide a quick look at the overall vibrational energy distribution as a function of frequency. Although this program is not normally used to establish modal damping coefficient information, it follows from equation (13) that this information might be deduced from a power spectral density function, using the one-half power method, if the input spectrum is broadband-flat. A typical power spectral density plot, obtained from the APSD program in analyzing the randomly excited response data contained in figure 2, is shown in figure 8.

The ENERGY, RESIDO, and COQUAD programs were primarily designed to evaluate swept frequency or random response data to detect whether any significant modes of vibration have been excited. If modes have been excited, these programs attempt to identify their number and to establish the damped natural frequency and damping coefficient of each detected mode. These programs are similar in that they all use a fast Fourier transform algorithm to compute a frequency response function. They differ in the way in which they manipulate this function to determine modal information.

If the test data contain a system driving function measurement, these programs can be directed to compute the cross-correlation function between system input/response quantities and the autocorrelation function of the system input. Transforming the resulting correlation information into the frequency domain and dividing the resulting cross-spectrum by the auto-spectrum results in a frequency response function representing the transfer function characteristics of the system under test. On the other hand, if the nature of the test data is consistent with the requirements of autocorrelation or random decrement signature analysis, the programs can compute frequency response information through the transformation of either one of these two functions. Although the frequency response functions computed from an autocorrelation function or a random decrement signature are somewhat different in form, they both can be considered representative of a transfer function characteristic possessing poles identical to the actual system under test.

System resonant frequency and damping coefficient information is determined in the COQUAD program by means of the frequency response component analysis method. Figures 9 and 10 show the amplitude and phase characteristics of a frequency response function computed by the COQUAD program in

analyzing simulated swept frequency velocity response data containing three modes (with damped natural frequencies of 3.0, 8.0, and 12.0 Hz and corresponding damping coefficients of 0.1, 0.1, and 0.2). Figures 11 and 12 show the in-phase and quadrature spectra of the calculated frequency response function. These figures are annotated to illustrate the component analysis computations implemented in the COQUAD program to determine the resonant frequency and damping coefficient information shown in the final program output tabulation. (See figure 13.) The ability of the COQUAD program to accurately determine system resonant frequency and damping coefficient information generally degrades as the modal frequency separation in the response data becomes small. For this reason, the program is primarily used to provide a supporting or alternate form of analysis in the actual reduction of flight test data. The COQUAD program is useful in applications where sufficient modal frequency separation exists.

The ENERGY and RESIDO programs provide the primary means of reducing frequency response information to determine the overall modal characteristics of the data. The modal identification process used by these two programs is similar. They both rectangularly window the calculated frequency response function and invert the windowed frequency domain information into the time domain. The windowed frequency response information reflects the response of a system having the calculated frequency response characteristic to an input signal having a rectangular frequency domain amplitude function with zero phase angle. The time domain form of this artifically created input signal is analytically computed and used along with the inverted response signal to determine system resonant frequencies and damping coefficients for those modes within the windowed frequency range using the LSDE algorithm. Digital band-pass filtering of the raw time domain signals is employed to minimize the effects of neighboring modes whose resonant frequencies are close to the windowed frequency range.

The differences between the ENERGY and RESIDO programs lie in the manner in which frequency response information is windowed and in the way the number of modes in a given window is established. The ENERGY program essentially scribes one or more lines across the calculated frequency response function at appropriate level(s) specified by the user. Generally, the intersection of the calculated frequency response function with these lines establishes the frequency windows to be used. The number of modes in each windowed section can be either automatically calculated or manually inserted after an examination of the frequency response function or its in-phase and quadrature spectrum. The number of modes in each window establishes the difference-equation model order to be used in the identification process. Conversely, the RESIDO program allows the user to segment the frequency response function into slightly overlapping windows spanning the entire frequency range of interest. These segments are individually inverted into the time domain where one or more user-specified models are used to determine the difference-equation coefficients corresponding to each window.

In both programs, the analytically determined difference-equation models essentially define Z-transfer function models (see equation (21)) pertaining

to various sections of the overall system frequency response function. These transfer function models are used to compute the energy of each mode calculated in each frequency window via a residue computation. Those modes whose resonant frequencies are within the windowed frequency range of the model and which, in addition, exceed some user selected level of significance are displayed on the primary output tabulation of the program. All computed modes, some of which can be mathematical fictions due to over-specified difference-equation model order, are output on a secondary program output tabulation. The final computation carried out by these programs is that of reconstructing the frequency response information from the mathematically determined Z-transfer functions. This reconstructed function can be compared to that previously calculated from the test data in order to ascertain the quality of the analytical fit. Examples of the excellent results, obtained in applying the ENERGY program to analysis of the clean swept frequency response data shown in figure 2, are set forth in figures 14 to 17. Results for the 42 Hz mode do not appear on the primary output tabulation because the energy of this mode was below the user selected level of significance for the test run. It should be noted that the correct answers were obtained for this mode, as indicated on the annotated secondary output tabulation in figure 16.

SOFTWARE INTERACTIVE CAPABILITIES

The on-line applications software used in the ATS is executed under control of the real-time TeleSCOPE 340 operating system. This system collects and stores data on a disk recall file over a total interval of time defined as a maneuver. Data analysis is implemented over maneuver sub-intervals called events. The flutter analysis programs selected by the user process event data from the disk. The operating system transfers data to the central computer on the request of the application program. In this manner, the analysis program is able to process data at a rate that is consistent with the requirements of its algorithm. Data can be processed in near-real-time, with the duration of analysis being a function of the complexity of the analysis technique.

At maneuver "initialization", the user has the ability to change or correct previously stored initialization information from the DAS console through the use of option displays which have been built into the various programs. The on-line flutter analysis programs require this interactive initialization capability in order to optimize analysis algorithms to suit the course of events occurring in a given flight. Before the flight, the analysis options are set to values which are considered adequate. In the case of the TLEFAD program this information is based on prior knowledge of the vehicle under test. Some analysis parameters are redefined after each maneuver, with less and less changes occurring as the flight progresses. For the RESIDO, ENERGY, and COQUAD programs, analysis options are initially set to much wider tolerances because of the broad overview analysis that is performed by these programs.

The most significant interactive capabilities associated with the use of the various flutter analysis programs are set forth in tables 1 and 2. Table

1 defines the system command options controlling the overall execution and displaying of program outputs from the DAS. An overview of the analysis options under the interactive control of the analyst are contained in table 2. Through the manipulation of these options, the analyst can generate a large volume of results. This can be a pitfall if not used prudently. For example, within the structure of the TLEFAD program a single frequency sweep can be analyzed for 14 different transducers using 2nd, 4th, and 6th ordered analysis, yielding a total of 84 separate frequency and damping answers to be evaluated. This is where experience is important, requiring judicious utilization of programs and options to avoid a deluge of results. However, from an overall flutter analysis point of view, the built-in ability to select different analysis program options enables the analyst to establish a high degree of confidence in the results obtained and increases the probability of a safe flutter buildup.

TEST RESULTS FROM SIMULATED DATA

The software on-line ability to accurately analyze flutter response data is best assessed by considering the results obtained in analyzing known test data simulating actual flight response characteristics. The results discussed herein were obtained by analyzing data from a highly coupled analog computer six-degree-of-freedom structural model. Clean and noisy swept frequency, as well as randomly excited response data generated by this model, was analyzed by the software in a normal flight-test configuration. This essentially consisted of feeding the analog test signals through the ATS facility where they were digitized and subsequently analyzed by various on-line programs. The results of this analysis were displayed on a CRT, at the Data Analysis Station, where they could be either copied to microfilm or hardcopy for record purposes. Analyzing the data in this manner reflects the normal processing errors associated with digitizing the data as well as the operational constraints of processing the data in a near-real-time environment.

Representative samples of the test data are shown in figure 2. The actual damped natural frequencies and structural damping coefficients of the six modes contained in these data are defined on figure 2. The random excitation used to drive the simulated system dynamics was generated by passing a broadband-flat noise source through a 3-Hz low-pass filter having a 6-dB per octave roll-off. In the noisy swept frequency configuration, the rms value of the model response to the noise input was approximately 6 volts. The rms value of the clean swept frequency response signal varied from 15 to 35 volts in the vicinity of the various resonances of the model. For the randomly excited test runs, the model was configured to achieve a reasonable contribution from all modes as indicated by the representative power spectral density plot of these data shown in figure 8.

Test results obtained by analyzing the clean and noisy swept frequency response data with the TLEFAD program, using the various preprocessing options available, are shown in table 3. These preprocessing options are denoted as direct analysis, cross-correlation analysis, and autocorrelation analysis and

reflect the respective utilization of the difference-equation models defined by equations (25), (26) and (28) for identification of modal resonant frequencies and damping coefficients. Data analysis for the various modes was initiated and terminated as a function of the frequency of the excitation signal. The frequency range over which data were analyzed for each mode or pair of modes is indicated in table 3 along with the filtering characteristics and difference-equation model order used in extracting the results. Overspecified difference-equation model orders were used to accommodate the presence of neighboring modes. The results quoted reflect the answers obtained for the known mode or modes within the pass-band of the digital filter used.

The results shown for the clean swept frequency are nearly perfect and reflect the answers obtained in a single run since there was little variability in the answers from run to run. Results quoted from the analysis of noisy data consist of the mean value plus and minus the one sigma standard deviation for system damped natural frequencies and damping coefficients that were obtained in analyzing data from ten independent shaker sweeps. These results indicate the superior noise rejection characteristics of the correlation methods, which tended to obtain results whose mean values were closer to the true modal values and which had less dispersion than those obtained via the direct analysis method, if a sufficient amount of data was available for averaging. The effect is seen in the test results by noting that the accuracy of the correlation results generally improved as modal frequency increased. This is a consequence of the exponential sweep function which increases the density of response data cycles as the frequency of the mode(s) increases. A confirmation of this was obtained by increasing the duration of the sweep and contrasting the significant improvement in the quality of the correlation results in the low frequency range with the minor changes in the upper frequency range where the amount of data previously analyzed was already sufficient for good results.

The randomly excited response data were analyzed via the RESIDO and TLEFAD programs. The TLEFAD program was set up to analyze the data via the autocorrelation preprocessing option, using the same filtering and modeling selections previously defined in the analysis of the swept frequency data. The only exception was that the data were analyzed over a specific time duration rather than a frequency range. These random data were also analyzed by the RESIDO program, using both the autocorrelation and random decrement signature methods over a frequency range of 1.6 to 57.0 Hz. The overall frequency range was uniformly segmented into four frequency intervals covering the approximate frequency ranges of 1.6 to 3.9, 3.9 to 9.5, 9.5 to 23.3, and 23.3 to 57.0 Hz. Fourth and sixth ordered difference-equation models were used to fit the overall frequency response function in each frequency segment. The results quoted herein reflect the utilization of the fourth ordered model in the lower two frequency ranges and the sixth ordered model in the upper two frequency ranges since the mathematically reconstructed frequency response information generally indicated that these models had achieved the best fit to the data.

Table 4 contains a summary of the results obtained in analyzing the randomly excited response data. Here again, a statistical summary of the results is presented, representing the mean value plus and minus the one

sigma standard deviation, for each set of runs. The number and duration of the runs for each set of results is appropriately indicated. In general, runs of equal duration were made over identical data sets, the only exception being that two less runs were made with the TLEFAD programs. Although only slightly evident in this set of runs, the results obtained by the TLEFAD program are generally better or equivalent to those obtained from the RESIDO program. This general trend is attributed to the fact that in operating the TLEFAD program the user takes advantage of his knowledge of the data modal composition to establish a more optimum selection of digital filtering characteristics and difference-equation model order. It should be noted that the 90-second duration results obtained from RESIDO indicate little difference between the autocorrelation and the random decrement signature methods and that the 180-second random decrement results show an improvement in overall accuracy due to increased time averaging. The random decrement signature level in all runs was set to the rms value of the first 4 seconds of data collected in each run.

TEST RESULTS FROM FLIGHT DATA

Typical time histories of the actual flight data analyzed are shown in figure 18. These data are grouped into the following frequency ranges and data types:

TYPE / RANGE	Clean	Noisy	Random	Bimodal
Less than 10 Hz (low)	Figure 18(a) Figure 18(b)	Figure 18(c)	Figure 18(d)	Figure 18(h) Figure 18(d)
10 Hz to 25 Hz (mid)	Figure 18(e)		-	-
Greater than 25 Hz (high)	Figure 18(f)	-	Figure 18(g)	-

A summary of the results is shown in table 5. The results shown are from the analysis of clean and noisy exponential sweeps (from 2 Hz to 70 Hz in 24 seconds) and from 90- to 180-second random excitations. The modes analyzed are characterized by the notation

(1) AW1B - antisymmetric wing first bending
(2) SW1B - symmetric wing first bending
(3) SW2B - symmetric wing second bending
(4) FLAPR - flap rotation
(5) W1B/STRP - wing first bending/store pitch

Before a detailed discussion of these results is presented, a few general comments are in order. The concept used in determining a tabulated number was the same as that used in the F-14A flutter program and is a result of the large capacity of the computer system and the program options available to the analyst. Specifically, these numbers are an average of the modal information obtained when the following program options (when

appropriate for the analysis method) were employed:

(1) Overspecification of analysis order
(2) Data analysis window variation
(3) Correlation lag range variation

In most cases 2nd, 4th and 6th ordered analysis was performed. If the number of results for a particular mode are less than six (which is considered a minimum for a statistical analysis), only the average result (without indication of the standard deviation) is tabulated.

Included are results from the TLEFAD program using the direct option which (see references 1 and 2 for additional discussion of results obtained using this analysis method) was the technique used during the F-14A flutter program. It is therefore considered to be the reference against which all other techniques are compared.

Considerable effort was spent on the analysis of the low frequency range, because realistic noise inputs such as buffet or gusts exhibit their highest spectral content in this range making it the most difficult frequency range to analyze.

Sweeps that are classified as clean do possess a certain minimal noise level but this is considered negligible compared to the other sweeps analyzed. The AW1B, SW1B, and FLAPR clean sweep, noisy sweep, and random noise data were obtained in level 1g flight at .85 Mach/25000 ft (1 ft = 0.3048 m). The noisy sweep and random data were obtained by holding the aircraft at 10° angle of attack at the given test condition, causing partial airflow separation and random excitation. Random flap excitation resulted from vorticies of the F-14A overwing fairing impinging on the flap. The SW2B sweep was obtained at .70 Mach/15000 ft, with the W1B/STRP sweep obtained at 1.05 Mach/6000 ft.

AW1B/SW1B Results

Analysis of the clean sweep AW1B results shows excellent agreement between the various techniques. The smallest standard deviation is with the TLEFAD cross-correlation option. The RESIDO cross-correlation scatter is higher because, in normal use, tight analysis control is not utilized with this program. As expected, all corresponding noisy sweep results had more scatter as exhibited by the greater standard deviations. However, the TLEFAD cross-correlation mean result is excellent, and the smaller scatter indicates the greater consistency that is achieved by utilizing the TLEFAD windowing philosophy in presence of noise relative to the wide windowing (overview) philosophy of RESIDO.

During random excitation both the AW1B and SW1B modes are excited, requiring TLEFAD direct results from both modes for reference purposes. The complete set of results shown for the AW1B mode reflects the consistency obtained using the different analysis techniques in the low frequency range.

Analysis of the SW1B mode was limited to clean sweep reference runs (using the direct and cross-correlation options in TLEFAD) for comparison with results obtained from randomly excited response data.

Because of the multimodal nature of the random response data only 4th and 6th ordered analysis results were considered. The TLEFAD autocorrelation 90- and 180-second results for the SW1B mode are good with slight improvement in results shown for the longer duration time slice. The AW1B results are not as good. However the trend again is favorable, the absolute error decreasing from 26% to 19% when the data duration time is doubled. The RESIDO autocorrelation and random decrement results are considered good for both modes with the exception of the SW1B frequency results.

SW2B Results

Data for the SW2B mode, which were acquired during 1g level flight, are classified as clean, but the response level is very low and it does possess a noise level which is greater than that of other clean sweeps. This is due to the location of the wing shaker near a SW2B node line which results in a low excitation level. Therefore it is felt that the true classification of this sweep lies between clean and noisy. Results for all the techniques utilizing the LSDE identification algorithm are consistent, establishing confidence in the utilization of all these techniques for flight data of such a low response level. The discrepancy between these results and those obtained from COQUAD is attributed to the decreased signal-to-noise ratio which had an adverse effect on this program.

FLAPR Results

The FLAPR results are sectioned into three distinct blocks each one associated with the clean sweep, noisy sweep, and random noise input. On the surface, it would appear that the programs are not capable of analyzing this mode because the frequency and damping results of each block are completely different. However examination of transfer function plots from the clean and noisy sweeps and power spectial density plots from the random excitation showed that the flap frequency and damping does change. It is believed that the different flap modal characteristics result because angle of attack changes increase static loading causing an increase in hinge moment. However, each block's results are consistent and it can be concluded that accurate identification for highly damped modes is a reality. This cannot be overlooked when explosive flutter mechanisms are being considered.

W1B/STRP Results

The final flight data discussed is a highly coupled bimodal response involving a classical W1B/STRP. Even though the data were acquired in a highly transonic region, the highly swept wing and sleek F-14A fuselage minimized transonic buffet effect, enabling it to be classified as clean.

These bimodal response data were analyzed with the TLEFAD program via the direct and cross-correlation methods and the RESIDO program using the cross-correlation method. The results for the three analysis techniques used are very consistent and varied little with changes in program options. No attempt was made to use COQUAD due to the inaccurate results normally obtained by the use of this program on bimodal response data. In all cases results for 6th ordered analysis models are presented because in this frequency range there is a 7-Hz fuselage vertical bending mode that is lightly reflected in the response data.

Experience gained in the analysis of simulated data indicates that accurate results are usually obtained when there is consistency between the different analysis methods. Extrapolating this trend to the results obtained here further confirms the fact that the LSDE identification algorithm is capable of successfully analyzing bimodal flight test data.

CURRENT DEVELOPMENTAL ACTIVITY

The Grumman LSDE identification approach is implemented in a manner that is predicated on linear systems theory. Occasionally, situations are encounted (most often due to mechanical effects) where response data manifest nonlinear behavior. The reduction of these data by linear techniques is difficult, if not impossible. Thus, it was decided to review existing analytical techniques that could provide a "nonlinear" analysis capability.

In recent years, various organizations have expended a considerable amount of effort in evaluating response-error modeling techniques for the purposes of extracting information on aircraft stability derivatives. (See references 3 and 4.) These techniques presume knowledge of the form for system dynamics, which is also a basic assumption of the LSDE identification approach used in reducing flutter response data. Grumman's current technique establishes system parameters by minimizing the mean-square equation-error resulting from the substitution of preprocessed data into an assumed difference-equation model. Response-error modeling techniques differ in that they determine system parameters by matching the response signal generated by an assumed dynamic model to actual response signal measurements so as to either minimize the error between them or increase the probability of obtaining good parameter estimates.

Since response-error modeling techniques can be implemented to analyze data from either linear or nonlinear systems, it was decided to direct an initial evaluation of the approach toward the more general problem of nonlinear system identification. In particular, the investigation was directed toward the evaluation of data from a nonlinear (hard-spring) resonant system. A detailed discussion of the technique, from the perspective of the example problem under investigation, is contained in Appendix B.

The basic approach consisted of implementing the technique so as to minimize the mean-square error between the actual and modeled systems. The

actual system was considered to have a nonlinear spring effect proportional to the square of displacement amplitude; the coefficient of the nonlinear spring was set at one-tenth of the value of the linear spring coefficient. Swept frequency runs were made for several different values of system damping coefficient. A discussion of the convergence problems encountered and how they were circumvented, by using algorithm constraints and initialization information inherent in the test data, is also contained in Appendix B.

The fundamental conclusions reached in this investigation indicated that the approach could be effectively used in the analysis of nonlinear response data. Plots showing the convergence of model parameters from their initially assumed values towards their true values are shown in figure 19. In general, it should be noted that the number of runs required to achieve convergence increased as the damping of the system decreased. This undesirable characteristic of the approach can probably be minimized through the utilization of second-order sensitivity coefficient terms and this will be pursued in subsequent investigations.

APPENDIX A

BASIC LINEAR SYSTEM CONCEPTS

This appendix contains a mathematical summary of the linear system concepts that form the basis for the algorithms used in the reduction of flight test flutter response data. The material is broken down into four sections. The first two deal with the underlying dynamic assumptions and linear system relationships that characterize system behavior. A derivation of the dynamic difference-equation modeling approximation that forms the basis for determining system resonant frequency and damping coefficient information is contained in the third section. The fourth section describes the least-squares identification algorithm used to determine difference-equation model coefficients and how these coefficients are processed to establish system resonant frequency and damping information.

Fundamental Stability Criteria

The ultimate objective of flutter test analysis is to measure or establish the relative margin of stability for the aeroelastic dynamics of an aircraft over its specified flight envelope. A basic assumption underlying Grumman's current on-line software analytics is that aircraft flutter dynamics are governed by a linear ordinary differential equation of the following form:

$$\sum_{n=0}^{N} d_n \frac{d^n y(t)}{dt^n} = \sum_{m=0}^{M} c_m \frac{d^m x(t)}{dt^m} \qquad (1)$$

where

$y(t)$ = displacement response (at some structural location)
$x(t)$ = structural driving function
d_n, c_m = constant coefficients (with $d_N = 1.0$)
N, M = positive integer constants ($M<N$)

If $Y(s)$ and $X(s)$ are used to denote the Laplace transforms of $y(t)$ and $x(t)$ it follows from equation (1), assuming the dynamic system is initially at rest, that

$$\frac{Y(s)}{X(s)} = H(s) = \frac{\sum_{m=0}^{M} c_m s^m}{\sum_{n=0}^{N} d_n s^n} = \frac{c_M \prod_{m=1}^{M} (s-z_m)}{\prod_{n=1}^{N} (s-p_n)} \tag{2}$$

where

$H(s)$ = dynamic system transfer function
z_m = zeros of H(s), roots of numerator polynomial
p_n = poles of H(s), roots of denominator polynomial

From the theory of linear systems, it is known that the dynamics equivalently defined by equation (1) or (2) are inherently stable if the characteristic roots of equation (1) or the poles of equation (2) lie in the left half of the complex plane. The aeroelastic dynamics of an aircraft structure represent a multi-degree-of-freedom system having resonant modes that can generally be related to those poles of H(s) which appear in complex conjugate pairs, such as

$$P_{2k} = -\alpha_k + i\beta_k \tag{3a}$$

$$P_{2k-1} = -\alpha_k - i\beta_k \tag{3b}$$

An aircraft encounters "flutter" or aeroelastic instability when α_k in equations (3a) and (3b) becomes negative. In practice it is common to refer to the damped natural frequency and structural damping coefficient of a given resonant mode. These particular variables are related to corresponding poles of H(s) by

$$g_k = \text{Structural damping coefficient of kth mode} = \frac{2\alpha_k}{(\alpha_k^2 + \beta_k^2)^{1/2}} \tag{4}$$

$$f_{dk} = \text{Damped natural frequency of the kth mode in Hz} = \frac{\beta_k}{2\pi} \tag{5}$$

As shown in equation (4), the structural damping coefficient of a mode is directly related to the real part of the modal pole and thus represents a measure of the stability of the corresponding mode under a given flight condition.

Underlying Background Relationships

Any analytical formulation of the solution to the problem of determining the natural frequencies and associated damping coefficient information from a response record implies a system model of the form defined in equation (1). Mathematical relationships used for the extraction of frequency and damping information can be implemented in a variety of ways. The actual method to be selected for a given application is strongly dependent on the nature of the test data to be analyzed. Several basic relationships pertaining to the system defined by equation (1) play an important role in either the implementation or understanding of analytical reduction algorithms applicable to different types of test data. Fundamentally the output of the linear system defined by equation (1) is uniquely determined from the knowledge of its impulse response function h(t) in accordance with the following time domain convolution integral:

$$y(t) = \int_{-\infty}^{+\infty} x(t-\sigma)h(\sigma)d\sigma \qquad (6)$$

where

$h(t)$ = the inverse Laplace transform of H(s), defined in equation (2)

If desired, the lower limit of integration in equation (6) can be changed from $-\infty$ to 0, since the subject system is causal (i.e., $h(t) = 0$ for $t<0$). This equation is possibly the most fundamental (least constrained) relationship characterizing linear system behavior. If x(t) and h(t) belong to the class of functions that are transformable, a useful frequency domain relationship can be obtained from equation (6) by taking its Fourier transform. The resulting equation is

$$Y(i\omega) = H(i\omega)X(i\omega) \qquad (7)$$

where

$Y(i\omega)$, $X(i\omega)$ = Fourier transforms of y(t) and x(t)
$H(i\omega)$ = System transfer function = $H(s)\big|_{s = i\omega}$

Equations (1), (2), (6), and (7) are all fundamental relationships that in themselves completely define system dynamic behavior.

Some interesting insights into test data analysis can be obtained by manipulation of equations (6) and (7). First if one filters the system response signal with a linear filter having a transfer function $F(i\omega)$ it follows that the filtered response signal is defined by

$$Y_f(i\omega) = Y(i\omega)F(i\omega)$$

which from equation (7) is seen to equal

$$Y_f(i\omega) = H(i\omega)X(i\omega)F(i\omega) = H(i\omega)X_f(i\omega) \tag{8}$$

where

$Y_f(i\omega)$, $X_f(i\omega)$ = Fourier transforms of filtered signals $y(t)$ and $x(t)$

Equation (8) states that the filtered response and driving function signals are dynamically related to each other through the same system transfer function as the unfiltered signals. Thus, in the analysis of system response to a known driving function, identically filtered measurements of system input and output data can be used without masking dynamic behavior. This filtering plays an important role in minimizing noise effects.

Certain well-known cross-correlation and cross-spectral relationships can be easily established along classical lines starting with either equation (6) or (7). The development here will emphasize those items considered significant in the computation of these functions for systems identification purposes. First consider the calculation of the cross-correlation of some arbitrary signal $w(t)$ with $y(t)$ and $x(t)$ over the finite interval of time ranging from t_1 to t_2 seconds as denoted by

$$\phi_{wy}(\tau) = \frac{1}{t_2 - t_1} \int_{t_1}^{t_2} w(t)y(t + \tau)dt \tag{9}$$

$$\phi_{wx}(\tau) = \frac{1}{t_2 - t_1} \int_{t_1}^{t_2} w(t)x(t + \tau)dt \tag{10}$$

Substituting y(t) from equation (6) into equation (9) results in the following cross-correlation convolution integral:

$$\phi_{wy}(\tau) = \frac{1}{t_2-t_1}\int_{t_1}^{t_2} w(t)\left[\int_{-\infty}^{+\infty} x(t+\tau-\sigma)h(\sigma)d\sigma\right]dt$$

$$= \int_{-\infty}^{+\infty} h(\sigma)\left[\frac{1}{t_2-t_1}\int_{t_1}^{t_2} w(t)x(t+\tau-\sigma)dt\right]d\sigma$$

$$= \int_{-\infty}^{+\infty} h(\sigma)\phi_{wx}(\tau-\sigma)d\sigma \qquad (11)$$

If the system is assumed to be initially at rest, it follows that both $\phi_{wy}(\tau)$ and $\phi_{wx}(\tau)$ are zero for $\tau<-t_2$ and that the upper limit of integration in equation (11) can be changed from $+\infty$ to $t_2+\tau$. Because the lower limit of integration can be set to zero, due to system causality, the resultant computation is finite. The majority of test situations involve the analysis of data from a stable system excited by a finite duration input signal. Under such conditions the correlation functions computed via equations (9) and (10) will tend to zero as τ increases in magnitude and thus represent functions whose Fourier transforms exist. Taking the Fourier transform of equation (11) results in the following cross-spectral relationship:

$$\Phi_{wy}(i\omega) = H(i\omega)\Phi_{wx}(i\omega) \qquad (12)$$

where

$\Phi_{wy}(i\omega)$, $\Phi_{wx}(i\omega)$ = Fourier transforms of $\phi_{wy}(\tau)$ and $\phi_{wx}(\tau)$

Comparing equation (11) with (6) and equation (12) with (7) reveals that the cross-correlation and spectral functions involved are mathematically related in the same manner as actual system input and output variables. Thus, an algorithm attempting to identify system resonant frequencies and damping coefficients from measured response and driving function signals can use cross-correlation or cross-spectral techniques to reduce the data without

disguising system characteristics. It should be noted that the above mentioned relationships hold regardless of the interval between t_1 and t_2. Obviously as this time interval increases, noise rejection improves and the calculated functions $\Phi_{wx}(\tau)$ and $\Phi_{wy}(\tau)$ become better approximations to their classical cross-correlation functions. Although cross-correlation and spectral techniques are slower from a computational point of view, they are more powerful in suppressing noise effects than simple filtering.

Autocorrelation and autospectral calculations, requiring only response signal measurements, can prove of value in analyzing flutter response data obtained from an aircraft excited by a driving function possessing an impulsive autocorrelation function. Random excitation having either a spectrum which is broadband-flat or one which can be considered as the output of a linear system which is driven by a broadband-flat random input satisfy this requirement. This random excitation can be obtained either naturally from a source such as atmospheric turbulence or artifically via random shakers. Deterministic signals such as a broadband sine wave sweep, a narrow spike, or function such as sine $(\omega t)/(\omega t)$, where ω is somewhat larger than the highest significant frequency in the response data, also satisfy the impulsive autocorrelation function requirements.

The mathematical significance underlying the autocorrelation approach can be evolved from either equation (6) or (7). Starting from equation (7), multiplying both sides of this equation by its complex conjugate results in

$$Y(-i\omega)Y(i\omega) = H(-i\omega)H(i\omega)X(-i\omega)X(i\omega)$$

or (13)

$$\Phi_{yy}(i\omega) = |H(i\omega)|^2 \Phi_{xx}(i\omega)$$

If $\Phi_{xx}(i\omega)$ is broadband-flat then

$$\Phi_{yy}(i\omega) \simeq |H(i\omega)|^2 = H(-i\omega)H(i\omega) \qquad (14)$$

Taking the inverse Fourier transform of equation (14) results in

$$\Phi_{yy}(t) = \int_{-\infty}^{+\infty} h(\tau)h(t + \tau)d\tau \qquad (15)$$

$$= \int_{-\infty}^{+\infty} h(-\tau)h(t - \tau)d\tau$$

Equation (15) indicates that the function $\phi_{yy}(t)$, which is essentially equivalent to the autocorrelation function of $y(t)$, is equal to a similar relationship representative of the autocorrelation function of $h(t)$. This equation also indicates that $\phi_{yy}(t)$ is equivalent to the system output response resulting from the input driving function equal to the impulse response function folded about the $t=0$ axis. For values of $t>0$ it follows that $\phi_{yy}(t)$ is actually the free decay of the system to the aforementioned input.

Another method for analyzing randomly excited response data, that has emerged in recent years, is the random decrement signature method. (See reference 5.) This method essentially averages fixed-duration segments of a random response record to obtain what is termed a random decrement signature. The particular segments to be selected and averaged from a given random response record are determined on the basis of signal level. Essentially, a predetermined level is established. Every time the amplitude of the response signal rises past or sinks below this level a fixed-duration segment of data, starting at the time the level is crossed, is averaged with previously accumulated segments. It can be reasoned that as the number of averaged segments increase the resultant random decrement signature will approach the free decay of the system from an initial displacement equal to the predetermined signature level. In some respects the random decrement signature is similar to an autocorrelation function in that both relationships represent free decay information. However these relationships are not equivalent since they represent different free decay problems.

Difference-Equation/Z-Transform Modeling Approximation

Grumman flutter analysis software uses what has been termed a model-matching method as a primary means of extracting resonant frequency and damping coefficient information from test data. Actually, the process is a least-squares equation-error parameter identification technique. In essence, coefficients or parameters of a dynamic model are analytically manipulated to obtain the best fit, in a least-squares sense, to the test data. The dynamic model used in the identification process takes the form of a finite-difference equation. This difference-equation model is a discrete version of equation (1) which is well suited for use in a digital computer where sampled values of test data must be dealt with. A detailed

derivation of this difference-equation model, accomplished through the use of Z-transform mathematics and sample-data system theory, is contained in reference 1. A somewhat abbreviated derivation is set forth below for the convenience of the reader.

The essence of the derivational approach is to model the continuous system with an open-loop sample-data system so that the synchronously sampled input and output signals of the modeled system approximately agree with their corresponding continuous system counterparts at the sampling instants. This is accomplished by assuming a sampled system model containing the continuous system transfer function H(s), as defined in equation (2), preceeded by a data reconstruction element possessing a polygonal hold characteristic.(See chapter 11, reference 6.) In the operational "s" notation of the Laplace transform, the transfer function for a polygonal hold reconstruction element is defined by

$$D(s) = \frac{e^{Ts}}{Ts^2}(1 - e^{-Ts})^2 \tag{16}$$

where

T = time increment between sampled data points

This data reconstruction element converts the sampled input to the model into a continuous signal constructed by connecting the sampled input points with straight lines. Driving the continuous system dynamics with this approximation to the actual input signal generally results in an output signal that agrees well with the actual system response signal, provided the sampling frequency is at least 5 times the upper pass-band limit of the continuous system and of a sufficient rate to insure a relatively smooth reconstructed input signal. The resultant transfer function for the modeled plant dynamics is

$$P(s) = D(s)H(s) \tag{17}$$

$$= \frac{(1-e^{-Ts})^2}{e^{-Ts}} H_1(s)$$

where

$$H_1(s) = \frac{1}{Ts^2} H(s)$$

The analysis of sample-data systems is generally accomplished through the use of the Z-transform in much the same manner as continuous systems analysis is tied together through the use of either the Laplace or Fourier transforms. The Z-transform represents a convenient means for handling sampled time functions. The Z-transfer function of a sample data system relates the Z-transforms of sampled system output to sampled system input and is simply converted to a time domain difference equation between sampled system input and output quantities. The Z-transfer function relationship for the modeled sample-data system is defined by

$$\frac{R(Z)}{X(Z)} = P(Z) \tag{18}$$

where

$R(Z)$ = Z-transform of sampled model output
$X(Z)$ = Z-transform of sampled input signal
$P(Z)$ = Z-transfer function of sampled data model
$Z = e^{Ts}$

Using the time shifting theorem, it follows from equation (17) that

$$P(Z) = \frac{(1 - Z^{-1})^2}{Z^{-1}} H_1(Z) \tag{19}$$

Now since $H_1(s)$ is expressible as a finite ratio of polynomials in s, whose denominator polynomial is of higher order than that of its numerator, it is possible to compute $H_1(Z)$ from $H_1(s)$ in accordance with the following integral definition of the Z-transform:

$$H_1(Z) = \sum_{\substack{\text{poles of} \\ H_1(s)}} \text{Res.} \left[H_1(s) \frac{1}{1-e^{Ts}Z^{-1}} \right] \tag{20}$$

Equation (20) expresses $H_1(Z)$ in terms of a sum of residues for the bracketed expression over the poles of $H_1(s)$. The result is that $H_1(Z)$ is expressible as a finite ratio of polynomials in Z. Substituting equation (20) into (19) and carrying out the indicated analytical manipulations, for the given form of $H_1(s)$, results in the following expression for P(Z):

$$P(Z) = \frac{\sum_{n=0}^{N} b_n Z^{-n}}{\prod_{n=1}^{N} (1-e^{p_n T} Z^{-1})} = \frac{\sum_{n=0}^{N} b_n Z^{-n}}{\sum_{n=0}^{N} a_n Z^{-n}} \tag{21}$$

Equation (21) shows that the Z-transfer function of the modeled sampled-data system is a finite ratio of polynomials in Z. The order of the numerator and denominator are both equal to N, which corresponds to the order of the denominator polynomial of H(s). This is a consequence of the data reconstruction device used and the assumed form of H(s). From equation (18) and (21) it follows that

$$R(Z) = -\sum_{n=1}^{N} a_n Z^{-n} R(Z) + \sum_{n=0}^{N} b_n Z^{-n} X(Z) \tag{22}$$

Taking the inverse Z-transform of equation (22) results in the following difference equation relationship:

$$r(t) = -\sum_{n=1}^{N} a_n r(t-nT) + \sum_{n=0}^{N} b_n x(t-nT) \tag{23}$$

where

r(t) = the inverse Z-transform of R(Z)

Equation (23) represents the dynamic difference-equation relationship between the modeled sample-data systems response r(t) and sampled values of the actual system input x(t). Since it is assumed that the modeled system response is approximately equal to the actual response of the continuous system at discrete sampling increments, this difference equation relationship is more appropriately written as

$$y(kT) = -\sum_{n=1}^{N} a_n y(kT-nT) + \sum_{n=0}^{N} b_n x(kT-nT) \tag{24}$$

where

k = a positive integer constant
y(kT), x(kT) = values of y(t) and x(t) at t=kT
a_n, b_n = constant difference equation coefficients corresponding to demonimator and numerator Z-transfer function polynomial coefficients

The a_n difference-equation coefficients in equation (24) are related to the poles p_n of the system transfer function H(s) as indicated in equation (21). System resonant frequencies and damping coefficients are determined from the poles of H(s) through the relationships defined in equations (3a) and (3b).

It follows from equation (8) that filtered system response and driving function data, $y_f(t)$ and $x_f(t)$, are related by the same general difference-equation relationship. Thus,

$$y_f(kT) = -\sum_{n=1}^{N} a_n y_f(kT - nT) + \sum_{n=0}^{N} b_n x_f(kT - nT) \qquad (25)$$

From equations (9) to (12), it obviously follows that the cross-correlation functions $\phi_{wy}(t)$ and $\phi_{wx}(t)$ are related in a similar fashion, resulting in

$$\phi_{wy}(kT) = -\sum_{n=1}^{N} a_n \phi_{wy}(kT - nT) + \sum_{n=0}^{N} b_n \phi_{wx}(kT - nT) \qquad (26)$$

If the system is excited by an input signal having a broadband-flat spectrum, the autocorrelation function of system response $\phi_{yy}(t)$ will be representative of the free decay of the system for values of t greater than zero. In this case, the following difference-equation relationship is implied:

$$\phi_{yy}(kT) = -\sum_{n=1}^{N} a_n \phi_{yy}(kT - nT) \qquad (27)$$

When dealing with response signals representing the free decay of the system, it follows from equation (24) that

$$y(kT) = \sum_{n=1}^{N} -a_n y(kT - nT)$$

It also follows that

$$w(jT)y(jT + kT) = \sum_{n=1}^{N} -a_n w(jT)y(jT + kT - nT)$$

where

j = a positive integer constant
w(t) = an arbitrary function of time

and, therefore,

$$\sum_{j=0}^{J} w(jT)y(kT + jT) = \sum_{j=0}^{J} \sum_{n=1}^{N} -a_n w(jT)y(jT + kT - nT)$$

or that, for the free decay problem, the following cross-correlation difference equation applies:

$$\phi_{wy}(kT) = \sum_{n=1}^{N} -a_n \phi_{wy}(kT - nT) \qquad (28)$$

Equations (25) to (28) represent those fundamental difference-equation relationships utilized by Grumman's on-line software for the purpose of identifying system resonant frequency and damping coefficient information.

Resonant Frequency/Damping Coefficient Identification

Equation (24) defines the basic difference-equation relationship used by Grumman's least-squares equation-error parameter identification algorithm. This equation will be used in the following analytical description of the technique although it should be understood that any of the difference equations represented by equations (25) to (28) could be used, as dictated by the manner in which the measured test data are initially processed.

Analytically, the least-squares equation-error identification technique minimizes the value of the function J shown below:

$$J = \sum_{k=k_1}^{k_2} (y_k - \bar{y}_k)^2 \tag{29}$$

where

k_1, k_2 = integer constants defining the data set over which J is to be minimized

y_k = y(kT) = the system response quantity at time kT

$\bar{y}_k$ = $\bar{y}$(kT) = the system response quantity estimated by the difference equation at time kT

In particular

$$\bar{y}_k = -\sum_{n=1}^{N} \bar{a}_n y_{k-n} + \sum_{n=0}^{N} \bar{b}_n x_{k-n} \tag{30}$$

where

$\bar{a}_n$, $\bar{b}_n$ = estimates of the a_n and b_n coefficients contained in equation (24) which minimize the function J

x(kT) = x_k = the system input quantity at time kT

If the system response signal is the only quantity required in data analysis, the second summation on the right-hand side of equation (30) is dropped.

The procedure for minimizing J consists of substituting equation (30) into equation (29) and taking the partial derivatives of the resulting expression with respect to the $\bar{a}_n$ and $\bar{b}_n$ coefficients, setting the expressions thus obtained to zero. This results in 2N+1 equations in 2N+1 unknowns which are to be solved for the desired coefficient information over the entire data set. The solution of these simultaneous linear equations, to obtain the desired estimates for difference-equation coefficients, can be expressed in the following matrix form:

$$\bar{K} = \{[B]^T[B]\}^{-1}\{[B]^T C\} \tag{31}$$

where

$$\overline{K} = \begin{bmatrix} -\overline{a}_1 \\ \vdots \\ -\overline{a}_N \\ \overline{b}_0 \\ \vdots \\ \overline{b}_N \end{bmatrix} \tag{32}$$

$$C = \begin{bmatrix} y_{k_1} \\ y_{k_1+1} \\ \cdot \\ \cdot \\ y_{k_2} \end{bmatrix} \tag{33}$$

$$[B] = \begin{bmatrix} y_{k_1-1} & \cdots & y_{k_1-N} & x_{k_1} & \cdots & x_{k_1-N} \\ y_{k_1} & \cdots & y_{k_1+1-N} & x_{k_1+1} & \cdots & x_{k_1+1-N} \\ \cdot & & \cdot & \cdot & & \cdot \\ \cdot & & \cdot & \cdot & & \cdot \\ \cdot & & \cdot & \cdot & & \cdot \\ y_{k_2-1} & \cdots & y_{k_2-N} & x_{k_2} & \cdots & x_{k_2-N} \end{bmatrix} \tag{34}$$

Equation (31) mathematically defines the identification process used in determining difference-equation coefficients. In this equation the superscripts T and -1 denote the respective matrix transpose and inverse operations.

Once the identification algorithm determines the $\overline{a}_n$ coefficients, as elements of the $\overline{K}$ vector, the roots of the denominator polynomial of the estimated Z-transfer function $P(Z)$ are computed. It follows from equation (21) that the roots of this polynomial are related to the estimated poles of H(s) by

$$\bar{\gamma} = e^{\bar{p}_n T} \tag{35}$$

where

$\bar{\gamma}$ = the nth root of the estimated Z-transfer function denominator polynomial
$\bar{p}_n$ = the estimated nth pole of H(s)

It can be seen from equation (35) that estimates for the real poles of H(s) are defined by

$$\bar{p}_n = \frac{1}{T} \ln (\bar{\gamma}_n) \tag{36}$$

From equations (3) and (35) it follows that estimates for the complex conjugate poles of H(s) are defined by

$$\bar{\gamma}_{2k} = e^{(-\bar{\alpha}_k T + i\bar{\beta}_k T)} = u_k + iv_k \tag{37a}$$

$$\bar{\gamma}_{2k-1} = u_k - iv_k \tag{37b}$$

and it follows that

$$-\bar{\alpha}_k = \frac{1}{T} \ln \sqrt{u_k^2 + v_k^2} \tag{38}$$

$$\bar{\beta}_k = \frac{1}{T} \left[\arctan \left(\frac{v_k}{u_k}\right) \right] \tag{39}$$

The real and imaginary parts of the complex conjugate poles of H(s) are computed in accordance with equations (38) and (39). The real poles of H(s) are computed from (36). System damped natural frequencies and damping coefficients are calculated from the real and imaginary parts of the complex conjugate poles of H(s) using the relationships shown in equations (4) and (5).

APPENDIX B

EXAMPLE NONLINEAR RESONANT SYSTEM IDENTIFICATION PROBLEM

The example problem described in this appendix depicts the application of the response-error modeling technique to the identification of a simplified nonlinear resonant system problem. The technique can be applied to the analysis of linear as well as nonlinear systems although it generally requires more computation time than the difference equation-error technique currently used by Grumman in the analysis of linear data. The utilization of response-error modeling techniques to linear and nonlinear system identification problems is currently undergoing extensive investigation, covering a broad range of scientific and engineering applications. Specific algorithms vary in complexity, generally depending on the manner in which model parameters are determined from response error.

The intent of the example described herein is to apply the concept, in its simplest form, to the analysis of resonant system phenomena typical of that which might be encountered in the analysis of flutter response data. The discussion set forth below is broken down into three sections. These sections respectively cover a statement of the example problem, a description of the analytical approach to be used in its solution and a discussion of some preliminary results obtained.

Problem Statement

The problem addressed here concerns itself with the identification of a nonlinear (hard-spring) resonant system defined by the following differential equation:

$$\ddot{Y}(t)+C_o\dot{Y}(t)+K_oY(t)+K_1\,\mathrm{sgn}[Y(t)]Y^2(t) = F(t) \qquad (40)$$

where

C_o, K_o, K_1 = constant parameters
$Y(t)$ = system displacement response
$F(t)$ = system forcing function
$\mathrm{sgn}[Y(t)]$ = +1 if $Y(t)$ is positive or
-1 if $Y(t)$ is negative

The constant parameters C_o, K_o, and K_1 determine the dynamic behavior of the system. Therefore, the identification process consists of defining the value of these parameters from measured data. It is assumed that relatively

clean measurements of system velocity response and forcing function are available. It is further assumed that the system is initially at rest and that the forcing function is a swept frequency sine wave whose frequency is varied from some point below to some other point above the apparent resonant frequency of the system.

The least-squares response-error modeling technique is to be used as the method for achieving system identification. This technique essentially assumes that the form of the dynamics are known, thus allowing the establishment of a dynamic system model. The identification process is implemented by varying the coefficients in the model so as to minimize the mean-square-error between the measured velocity response of the actual system and the corresponding velocity response of the assumed model.

Underlying Analytical Approach

Since knowledge of the actual system's form is assumed, the following equation defines the system model:

$$\ddot{y}(t)+c_o\dot{y}(t)+k_o y(t)+k_1 \operatorname{sgn}[y(t)]y^2(t) = F(t) \tag{41}$$

The lower-case nomenclature used in equation (41) distinguishes modeled system quantities from those of the actual system, as defined by equation (40). Starting with initial estimates for c_o, k_o, and k_1, along with measured values of system driving function, equation (41) is solved to obtain its velocity response over some interval of interest. Model parameters are incremented, from run to run, so as to minimize the following mean square error function:

$$J = \int_0^T E^2(t)\, dt \tag{42}$$

where

T = time duration of analysis

$E(t) = \dot{Y}(t)-\dot{y}(t)$

In order to analytically compute the parameter changes required to minimize J it is necessary to express $\dot{y}(t)$ as a function of these quantities. For a given forcing function, $\dot{y}(t)$ can be considered to be a function of its current parameter values (i.e., c_o, k_o, and k_1) and time. The form of $\dot{y}(t)$ for some other set of parameter values (i.e., $c_o + \Delta c_o$, $k_o + \Delta k_o$ and $k_1 + \Delta k_1$) can be simply approximated from the first order terms of the Taylor series expansion for $\dot{y}(t)$ as indicated in the following equation:

$$\dot{y}_\Delta \approx \dot{y}_o + \frac{\partial \dot{y}_o}{\partial c_o} \Delta c_o + \frac{\partial \dot{y}_o}{\partial k_o} \Delta k_o + \frac{\partial \dot{y}_o}{\partial k_1} \Delta k_1 \tag{43}$$

where

$$\dot{y}_o = \dot{y}(c_o, k_o, k_1, t)$$
$$\dot{y}_\Delta = \dot{y}(c_o + \Delta c_o, k_o + \Delta k_o, k_1 + \Delta k_1, t)$$

The partial derivatives of the right-hand side of equation (43) are time varying sensitivity coefficients which are solutions to sensitivity differential equations. These differential equations are easily derived from equation (41) by taking the partial derivative of this latter equation with respect to each parameter as indicated below:

$$\frac{\partial \ddot{y}_o}{\partial c_o} = \frac{d^2}{dt^2} \frac{\partial y_o}{\partial c_o} = \frac{\partial}{\partial c_o} [-c_o \dot{y}_o - k_o y_o - k_1 \operatorname{sgn}(y_o) y_o^2 + F(t)]$$

$$= -c_o \frac{d}{dt} \frac{\partial y_o}{\partial c_o} - k_o \frac{\partial y_o}{\partial c_o} - 2k_1 \operatorname{sgn}(y_o) y_o \frac{\partial y_o}{\partial c_o} + \cancelto{0}{\frac{\partial F(t)}{\partial c_o}} - \dot{y}_o$$

which can be written as

$$\ddot{S}_1 + c_o \dot{S}_1 + [k_o + 2k_1 \operatorname{sgn}(y_o) y_o] S_1 = -\dot{y}_o \tag{44}$$

where

$$S_1 = \frac{\partial y_o}{\partial c_o}$$

In a like manner the sensitivity equations for k_o and k_1 are defined by

$$\ddot{S}_2 + c_o\dot{S}_2 + [k_o + 2k_1 \text{sgn}(y_o)y_o]S_2 = -y_o \tag{45}$$

$$\ddot{S}_3 + c_o\dot{S}_3 + [k_o + 2k_1 \text{sgn}(y_o)y_o]S_3 = -\text{sgn}(y_o)y_o^2 \tag{46}$$

where

$$S_2 = \frac{\partial y_o}{\partial k_o}$$

$$S_3 = \frac{\partial y_o}{\partial k_1}$$

Equations (44), (45), and (46) are linear, second-order, differential equations with time varying stiffness coefficients that are a function of the modeled system's displacement signal. The excitation signals driving the sensitivity differential equations are a function of the velocity or displacement response of the modeled system. The time varying sensitivity coefficients required in equation (43) are obtained by solving equations (44) to (46) along with equation (41).

Now that all the elements in equation (43) are defined, it can be substituted into equation (42) resulting in

$$J = \int_0^T [\dot{Y} - \dot{y}_o - \dot{S}_1\Delta c_o - \dot{S}_2\Delta k_o - \dot{S}_3\Delta k_1]^2 dt \tag{47}$$

The function J is minimized by taking its partial derivative with respect to each of the incremental parameter changes and setting the resulting expressions to zero. The solution of the three simultaneous linear equations,

to obtain the three incremental parameter changes, can be expressed in the following matrix form:

$$P = [S]^{-1}V \tag{48}$$

where

$$P = \begin{bmatrix} \Delta c_o \\ \Delta k_o \\ \Delta k_1 \end{bmatrix} \tag{49}$$

$$V = \int_0^T \begin{bmatrix} \dot{S}_1(Y-y_o) \\ \dot{S}_2(Y-y_o) \\ \dot{S}_3(Y-y_o) \end{bmatrix} dt \tag{50}$$

$$[S] = \int_0^T \begin{bmatrix} \dot{S}_1^2 & \dot{S}_1 S_2 & \dot{S}_1 S_3 \\ \dot{S}_2 S_1 & \dot{S}_2^2 & \dot{S}_2 S_3 \\ \dot{S}_3 S_1 & \dot{S}_3 S_2 & \dot{S}_3^2 \end{bmatrix} dt \tag{51}$$

The elements of the P vector, computed by multiplying the inverse S matrix by the V vector, express the parameter changes resulting from a given pass through the data. The process is generally repeated until the parameter changes become small or the calculated value of J falls below some prescribed level.

Example Problem Results

A digital-computer algorithm using the defined analytical approach was designed for the purposes of making a preliminary evaluation of the technique. In this evaluation the K_o and K_1 system parameters were set at numerical values of 3948 and 394.8, with the value of C_o being varied

between 3.142 and 12.57. A linear system with these values for C_o and K_o would have a resonant natural frequency of 10 Hz and structural damping coefficients ranging from 0.05 to 0.2. The apparent resonant frequency of the actual nonlinear (hard-spring) system is generally higher than 10 Hz increasing with the magnitude of system displacement. This, in turn, is a function of the system's inherent damping and the magnitude of the driving function. The assumed form of the driving function was an exponential swept frequency sine wave covering the 6 to 20 Hz frequency range in approximately 6 seconds. The amplitude of the driving function was held at a constant amplitude which was numerically equivalent to K_o.

Initial runs indicated that convergence of the algorithm was dependent on having reasonable initial estimates for system parameters. In practice good estimates are not always available. Rather than increasing the analytical complexity of the coefficient updating technique, which was considered outside the scope of this preliminary investigation, it was decided to adopt a strategy that could be applied in practice, with suitable constraints, to generally insure convergence. The strategy adopted was based on the inherent information contained in the test data and the user's presumed knowledge for the form of the system's dynamics. In accordance with this strategy, the initial value of k_1 was set to zero, with the initial value of k_o taken as the squared value of the apparent resonant frequency of the response data. This frequency is simply determined by measuring the period of the response signal in the vicinity of its peak value. The initial value for c_o was selected at a tenth of the square root of k_o. This would correspond to a nominal structural damping coefficient of 0.1 if the system were linear.

Algorithm parameter updating was constrained so that k_1 would be set back to zero if its value went negative or became greater than the current value of k_o. The value of k_o was prevented from falling below a tenth of its initial value. Finally, the parameter changes from run to run were constrained so that the change in k_o could not exceed the initial value of k_o and that the change in k_1 could not exceed a tenth of the initial value of k_o. If either or both of these parameter changes exceed their corresponding limits all parameter changes were uniformly attenuated by a factor (not to be less than a tenth) in an attempt to prevent any parameter change from exceeding its limit. For the problem at hand, the above constraints are considered loose and were determined empirically with no attempt being made to refine them in an optimal sense.

Using this strategy, results were obtained in analyzing data from systems having C_o damping terms of 12.57, 6.283, and 3.141. The stiffness

coefficients K_o and K_1 were held at constant values of 3948 and 394.8. The results listed below reflect the ability of the approach to converge on the true coefficient values with the inherent characteristic of requiring more iterations as damping decreases.

	Analysis Pass	Model Parameter c_o	k_o	k_1
For C_o = 12.57	0	6.911	4777.	0.0
	1	11.70	4724.	35.56
	2	14.32	4411.	217.4
	3	12.87	3843.	439.6
	4	12.67	3977.	386.2
	5	12.57	3947.	395.2
	6	12.57	3948.	394.8
For C_o = 6.283	0	7.540	5685.	0.0
	1	10.51	4644.	323.6
	2	6.423	4618.	391.0
	3	8.113	4914.	387.5
	4	8.337	5136.	262.5
	5	6.139	4151.	394.0
	6	6.832	4482.	343.3
	7	6.458	4157.	368.3
	8	6.294	3943.	397.5
	9	6.282	3948.	394.7
	10	6.283	3948.	394.8
For C_o = 3.141	0	8.796	7738.	0.0
	1	5.727	5803.	474.2
	2	5.960	4981.	605.8
	3	4.738	6064.	260.7
	4	2.967	5557.	235.6
	5	3.244	5630.	234.8
	6	3.280	5359.	263.3
	7	3.284	5066.	293.7
	8	3.306	4745.	328.0
	9	3.281	4300.	372.9
	10	3.171	3979.	396.1
	11	3.137	3954.	394.1
	12	3.140	3949.	394.6
	13	3.141	3948.	394.8

REFERENCES

1. Waisanen, P.R., and Perangelo, H.J.: Real Time Flight Flutter Testing via Z-Transform Analysis Technique. AIAA Paper No. 72-784, 1972.

2. Baird, E.F., and Clark, W.B.: Recent Developments in Flight Flutter Testing in the United States. Paper presented at 34th meeting of AGARD Structures and Materials Panel, Lyngby, Denmark, April 1972.

3. Taylor, Lawrence W.,Jr., and Iliff, Kenneth W.: Systems Identification using a Modified Newton-Raphson Method - A FORTRAN Program. NASA TN D-6734, May 1972.

4. Grove, Randell D., Bowles, Roland L., and Maybew, Stanley C.: A Procedure for Estimating Stability and Control Parameters from Flight Test Data by using Maximum Likelihood Methods Employing a Real-Time Digital System. NASA TN D-6735, May 1972.

5. Cole, Henry A., Jr.: On-Line Failure Detection and Damping Measurement of Aerospace Structures by Random Decrement Signatures. NASA CR-2205, March 1973.

6. Ragazzini, J.F., and Franklin, G.F.: Sampled-Data Control Systems. McGraw-Hill Book Company, Inc., New York, 1958.

Table 1.- System command options

Item	Input*	Function
Maneuver mode	KB	Application program selection
Plot menu	LK, LP	Selects plots and/or tabs for display
Start maneuver	LK	Initiates real time data transfer to disk
Start event	LK	Initiates processing and tagging of data
Stop event	LK	Tags end of data slice to be processed
Stop maneuver	LK	Ends disk recording and processing
Recall mode	KB, LK	Allows intermaneuver disk data processing
Plot recall	KB, LP	Allows display of previous analysis results
Utility option	KB, LP	Enables access to files for purposes of changing plot scales, data scaling and certain program analysis variables

* Input types: KB - Keyboard type-ins
LK - Latchkey push button selection
LP - Display light pen selection

Table 2.- Overview of major analysis program options

Item	Analysis options
Model analysis order	Model order can be varied from 2 up to 14 for each response transducer
Multiple analysis order	Multiple ordered analysis models can be specified for use on response data yielding separate results
Data preprocessing	Recusive digital filtering, cross-correlation analysis, autocorrelation analysis, or random decrement signature processing
Filtering control	Specification of pass-band and roll-off characteristics (up to 36 dB per octave)
Correlation lag range	Selection of correlation function positive and negative lag range
Transform size	Fast Fourier transform size up to 2048 points
Data window	Specification of time duration or frequency range
Transducer selection	Analysis of 1 to 28 measurements at 500 samples per second
Data sample rate	500, 250,or 100 samples per second

Table 3. - Summary of TLEFAD results on simulated swept frequency response data

TLEFAD pre-processing option	Analysis results*				Data analysis window	Filter pass-band	Model order
	Clean		Noisy				
	f_d	g	$f_d \pm 1\sigma$	$g \pm 1\sigma$			
Direct	2.00 3.00	.100 .050	2.01±.026 3.06±.050	.092±.018 .038±.013	1.6 to 3.6 Hz	1.5 to 3.9 Hz	6
	8.01	.075	7.95±.055	.078±.022	7.0 to 9.0 Hz	6.0 to 10.5 Hz	4
	16.0	.031	16.0±.032	.033±.007	14.0 to 18.0 Hz	12.0 to 19.0 Hz	4
	42.6 52.2	.189 .053	37.4±1.10 51.6±.404	.100±.023 .083±.007	33.6 to 54.6 Hz	33.0 to 67.0 Hz	6
Cross-correlation	2.00 3.00	.100 .050	2.00±.023 3.01±.018	.093±.019 .048±.011	1.5 to 4.5 Hz	0.0 to 3.9 Hz	6
	8.01	.075	7.99±.043	.073±.012	6.0 to 10.0 Hz	6.0 to 10.5 Hz	4
	16.0	.030	16.0±.000	.030±.002	12.0 to 20.0 Hz	12.0 to 19.0 Hz	4
	41.8 52.0	.198 .050	41.0±.468 52.0±.052	.220±.024 .050±.001	35.0 to 59.0 Hz	33.0 to 67.0 Hz	6
Auto-correlation	1.99 3.00	.104 .050	2.00±.025 3.01±.023	.077±.024 .037±.008	1.5 to 12.0 Hz	1.5 to 3.9 Hz	6
	8.00	.075	8.01±.139	.072±.030	4.0 to 12.0 Hz	6.0 to 10.5 Hz	6
	16.0	.031	16.0±.032	.028±.003	10.0 to 22.0 Hz	10.0 to 19.0 Hz	4
	41.8 52.1	.198 .050	41.5±.239 52.1±.048	.203±.011 .050±.002	26.0 to 62.0 Hz	33.0 to 67.0 Hz	6

* f_d = damped natural frequency of mode

g = structural damping coefficient of mode

σ = standard deviation

Table 4. - Summary of results on simulated randomly excited response data

Program	Option	Time duration (seconds)	Number of runs	True results		Analysis results	
				f_d	g	$f_d \pm 1\sigma$	g $\pm 1\sigma$
TLEFAD	Auto-correlation	90	11	2.00	.100	2.00±.042	.084±.019
				3.00	.050	3.00±.024	.041±.011
				8.00	.075	8.01±.055	.063±.017
				16.0	.030	16.0±.060	.031±.006
				42.0	.200	41.6±1.03	.182±.029
				52.0	.050	52.1±.149	.051±.004
RESIDO	Auto-correlation	90	13	2.00	.100	2.01±.034	.068±.015
				3.00	.050	3.01±.017	.041±.012
				8.00	.075	8.01±.052	.067±.016
				16.0	.030	16.0±.055	.025±.004
				42.0	.200	42.1±.380	.186±.024
				52.0	.050	52.2±.168	.052±.006
	Random decrement	90	13	2.00	.100	2.00±.037	.068±.023
				3.00	.050	3.00±.029	.041±.015
				8.00	.075	8.02±.060	.059±.017
				16.0	.030	16.0±.073	.027±.005
				42.0	.200	42.6±.526	.194±.044
				52.0	.050	53.4±.307	.055±.007
		180	6	2.00	.100	2.00±.021	.076±.009
				3.00	.050	3.01±.018	.045±.010
				8.00	.075	8.03±.051	.058±.011
				16.0	.030	16.0±.049	.027±.002
				42.0	.200	42.5±.407	.185±.026
				52.0	.050	52.3±.157	.053±.006

Table 5. - Summary of flight test data results

	Mode / Analysis	AW1B		SW1B		SW2B		FLAPR		W1B/STRP	
		f_d σ	g σ	f_d σ	g σ	f_d σ	g σ	f_d σ	g σ	f_d W1B f_d STRP	g W1B g STRP
clean sweep	TLEFAD	6.15	.089	5.26	.134	15.2	.097	48.1	.251	6.46	.107
	direct	.097	.011	.080	.022	.197	.008	2.44	.028	7.74	.080
	TLEFAD	6.15	.095	5.24	.139	15.2	.103	49.3	.252	6.44	.101
	cross-corr	.035	.007	.055	.014	.155	.009	.652	.007	7.76	.079
	RESIDO	6.14	.086	-	-	15.1	.082	49.8	.238	6.45	.104
	cross-corr	.143	.036	-	-	.358	-	1.84	.028	7.67	.071
	COQUAD	6.10	.117	-	-	14.8	.124	49.5	.227	-	-
		-	-	-	-	-	-	-	-	-	-
noisy sweep	TLEFAD	5.91	.100	-	-	-	-	-	-	-	-
	direct	.308	.035	-	-	-	-	-	-	-	-
	TLEFAD	6.12	.103	-	-	-	-	54.2	.063	-	-
	cross-corr	.230	.027	-	-	-	-	-	-	-	-
	RESIDO	6.17	.093	-	-	-	-	54.4	.073	-	-
	cross-corr	.320	.040	-	-	-	-	-	-	-	-
90 sec. random	TLEFAD	6.04	.066	5.20	.117	-	-	-	-	-	-
	autocorr	-	-	-	-	-	-	-	-	-	-
	RESIDO	6.02	.109	5.76	.107	-	-	59.5	.215	-	-
	autocorr	-	-	-	-	-	-	-	-	-	-
	RESIDO	6.03	.102	5.69	.094	-	-	58.7	.197	-	-
	random-dec	-	-	-	-	-	-	-	-	-	-
180 sec. rand.	TLEFAD	6.15	.106	5.19	.124	-	-	-	-	-	-
	autocorr	-	-	-	-	-	-	-	-	-	-
	RESIDO	6.07	.076	5.67	.161	-	-	-	-	-	-
	autocorr	-	-	-	-	-	-	-	-	-	-

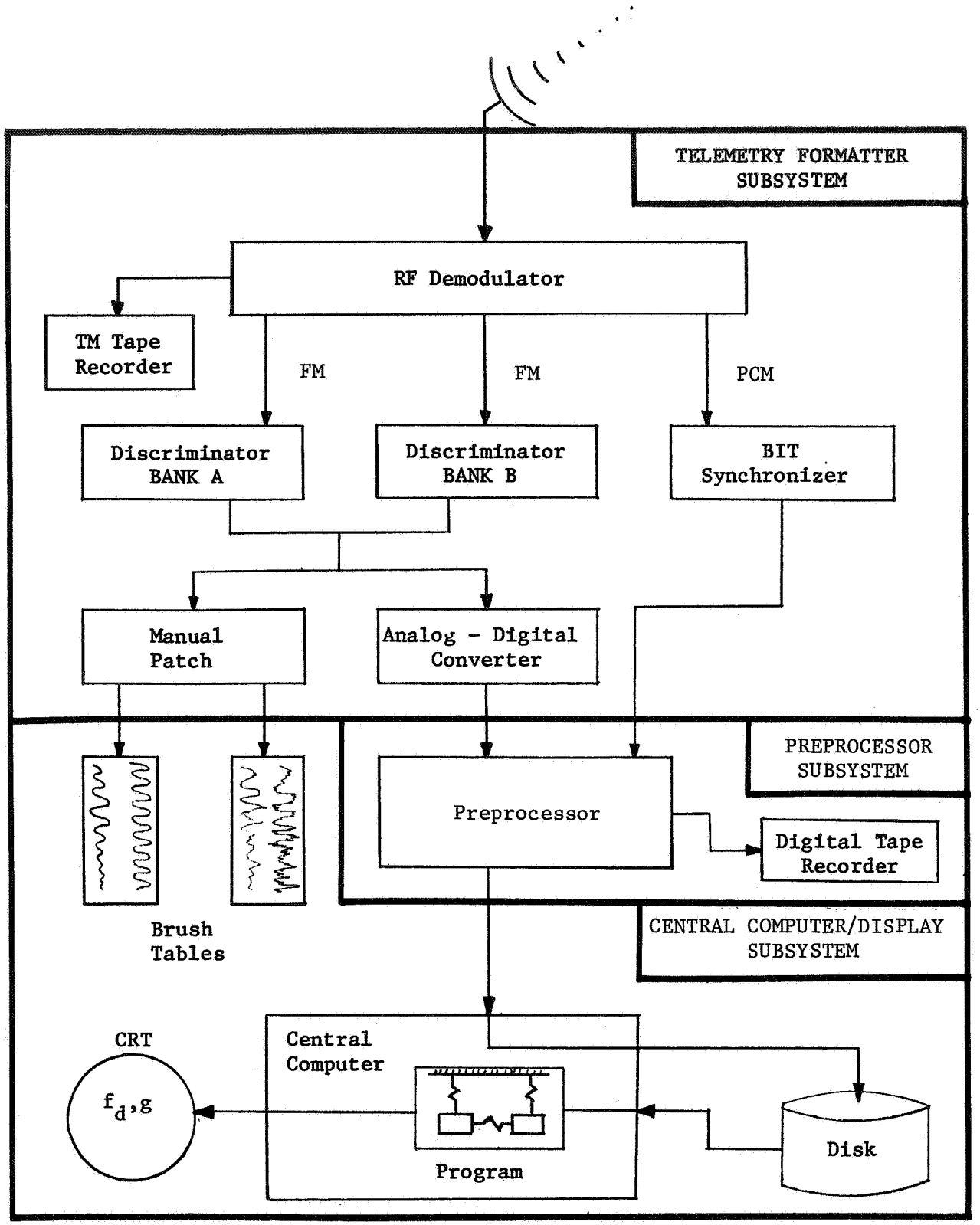

Figure 1. - Block diagram of Automated Telemetry Station.

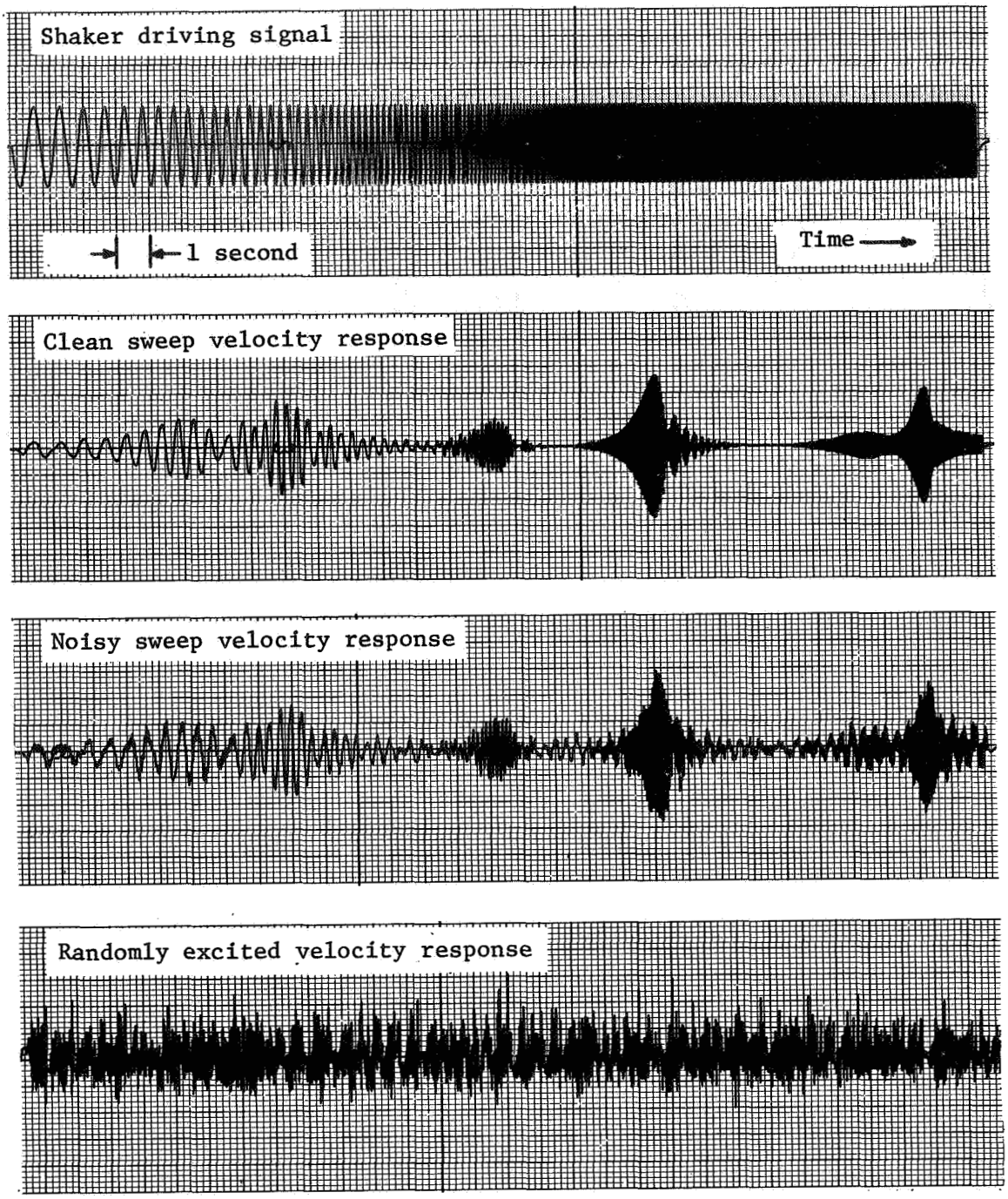

Modal characteristics: freq.= 2.00 - 3.00 - 8.00 - 16.0 - 42.0 - 52.0
damp.= .100 - .050 - .075 - .030 - .200 - .050

Figure 2.- Simulated flutter response data.

MODE - IDENTITY			PRIMARY XDUCER F-1	PRIMARY XDUCER G-1	SECONDARY XDUCER F-2	SECONDARY XDUCER G-2	KEAS	MT	MPT	EVENT TIME
M0210	0	1	2.00	0.083						9.6040
M0305	0	1	2.97	0.058						9.6040
M0011		1	-1.5	-1.50						9.6040
?	?	1	0.06	-1.00						9.6040
M0807	5	2	4.94	1.264						15.172
M08DU	M	2	8.00	0.070						15.172
M1603	0	3	12.2	0.561						20.096
M16DU	M	3	15.9	0.029						20.096
M4220	0	4	0.02	-1.00	0.000	590.5	0.93	1515.2		27.908
M5205	0	4	0.00	-1.00	0.000	590.5	0.93	1515.2		27.908
M0014		4	40.8	0.188	0.000	590.5	0.93	1515.2		27.908
?	?	4	51.9	0.052	0.000	590.5	0.93	1515.2		27.908

Resonant frequency - damping coefficient results obtained from noisy sweep in figure 2.

Figure 3. - Annotated primary output tabulation from TLEFAD program.

MODE -- ID			PRI CHAN	SEC CHAN	PRI ERROR FACTOR	SEC ERROR FACTOR	ACTUAL DATA--LOAD	ACTUAL FA	ACTUAL FB
M0210	0	1	15	99	1.598-4	00000	0059	1.49	4.50
M0807	5	2	15	10	2.566-4	1.630-6	0032	5.99	10.0
M1603	0	3	15	19	1.650-6	5.617-8	0120	11.9	20.0
M4220	0	4	15	99	1.108-6	00000	0001	54.9	59.0

Figure 4. - Validation output tabulation from TLEFAD program.

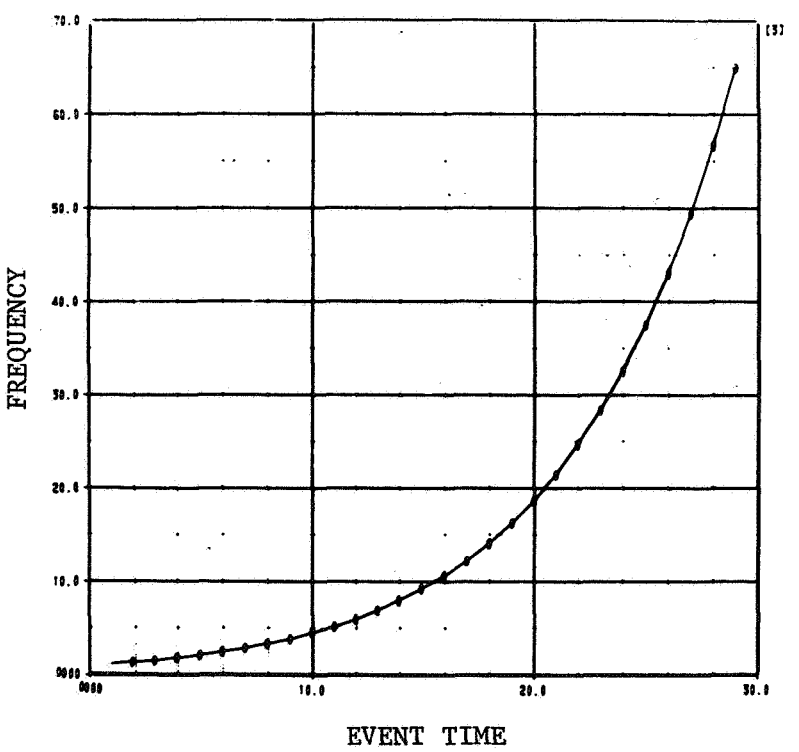

Figure 5. - Shaker frequency plot from TLEFAD program.

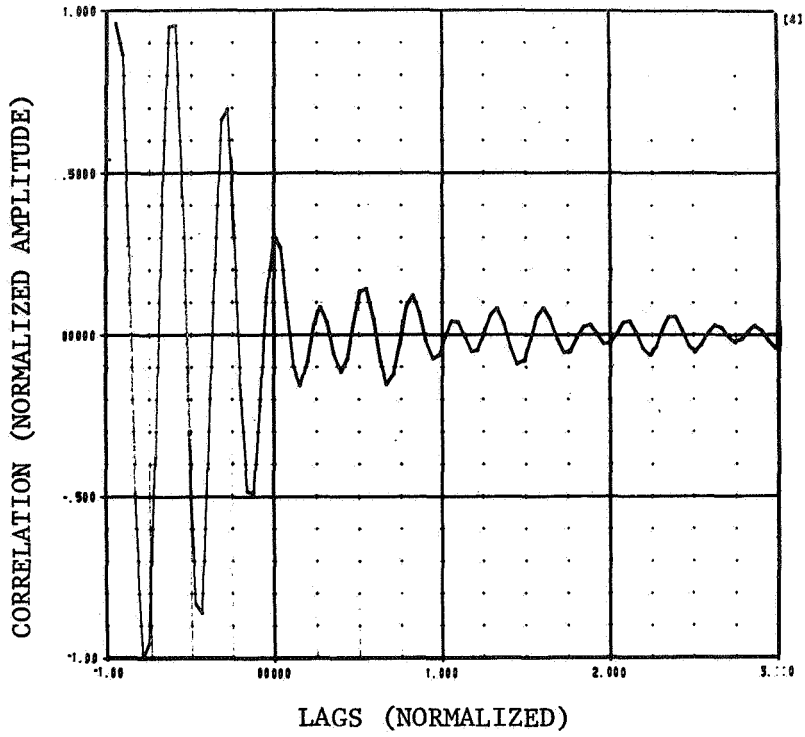

Figure 6. - Input signal cross-correlation function from TLEFAD program.

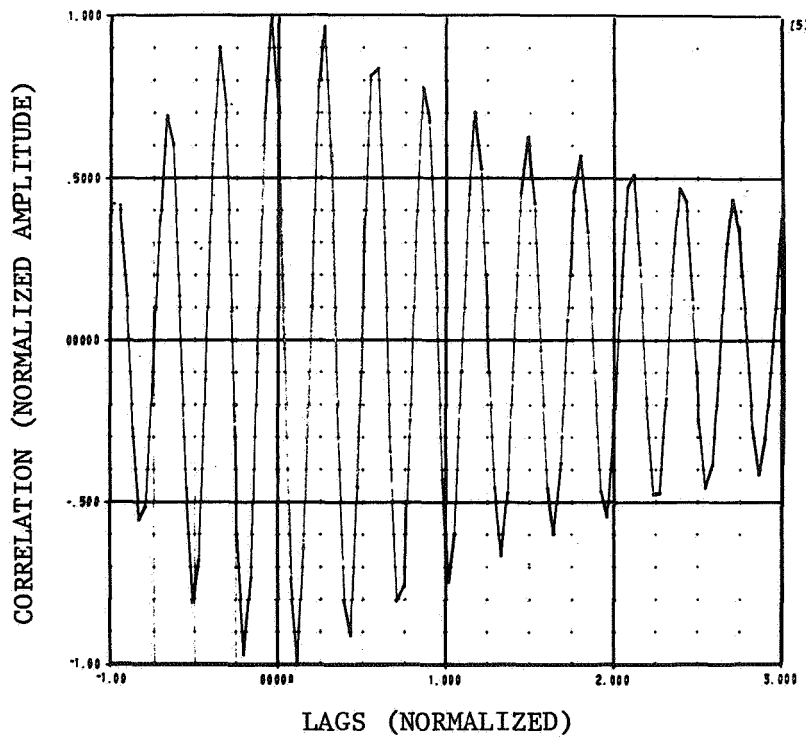

Figure 7. - Response signal cross-correlation function from TLEFAD program.

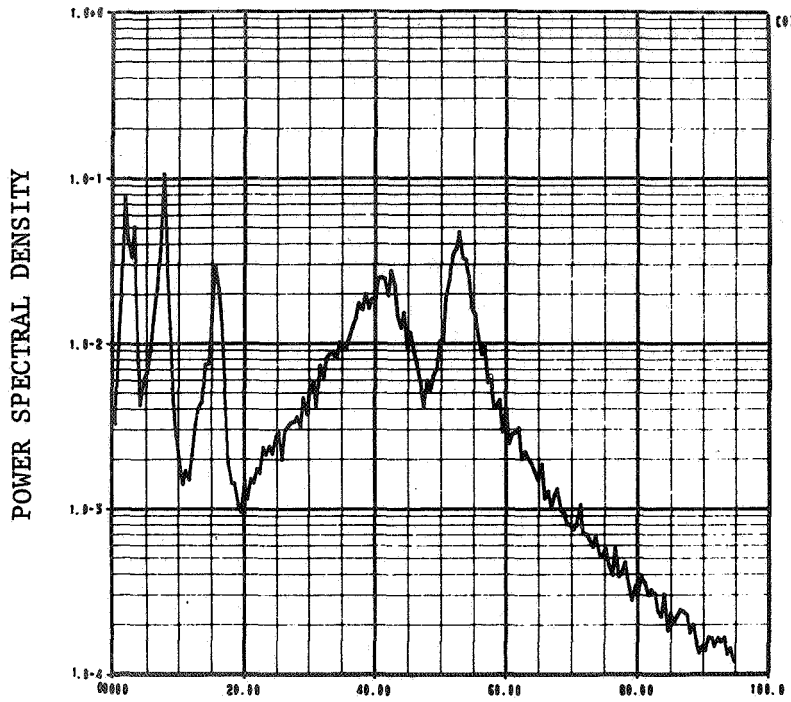

Figure 8. - Power spectral density plot from APSD program.

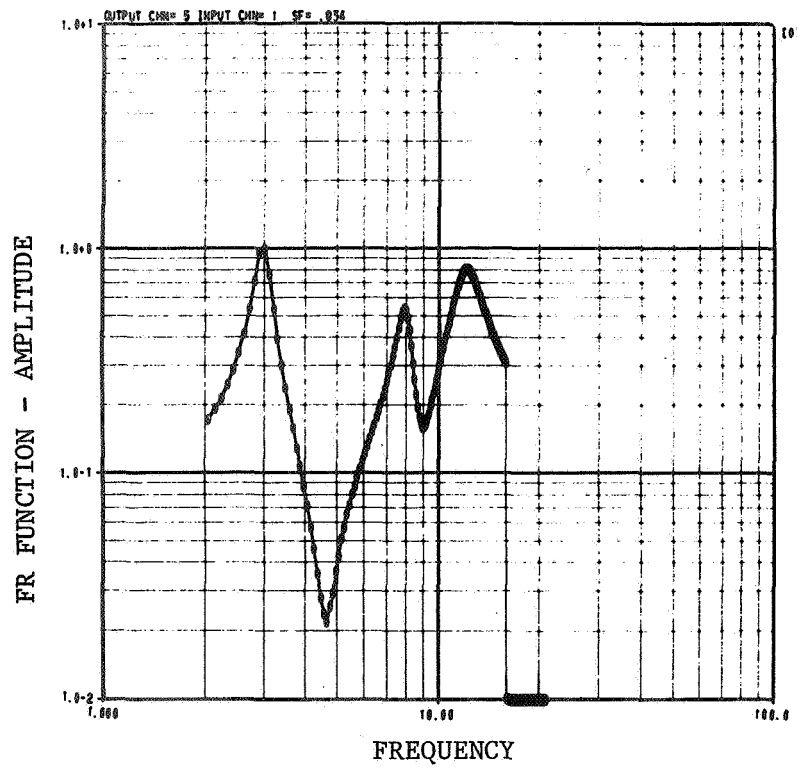

Figure 9. - Frequency response function amplitude from COQUAD program.

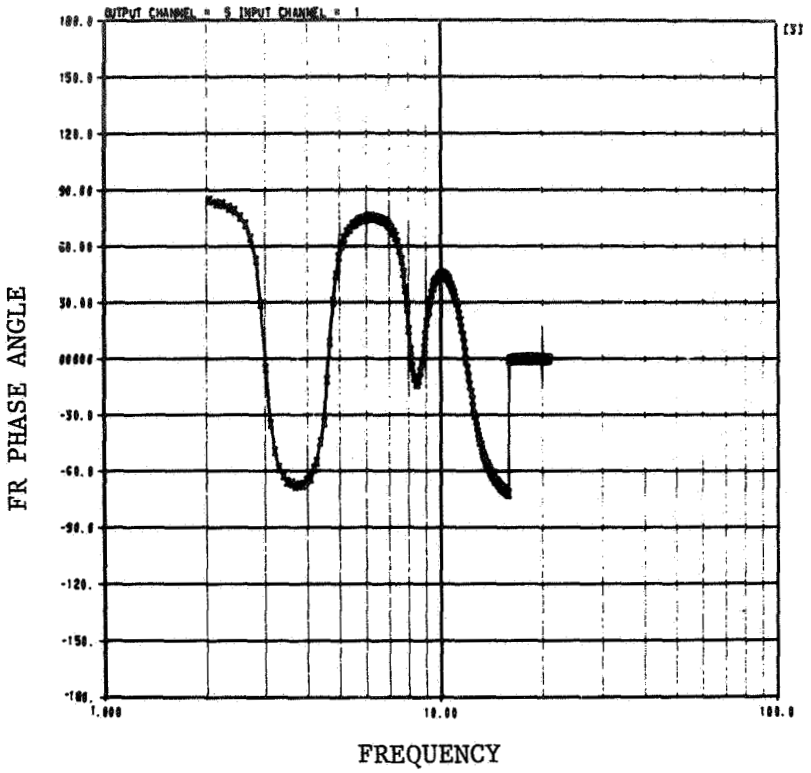

Figure 10. - Frequency response phase angle from COQUAD program.

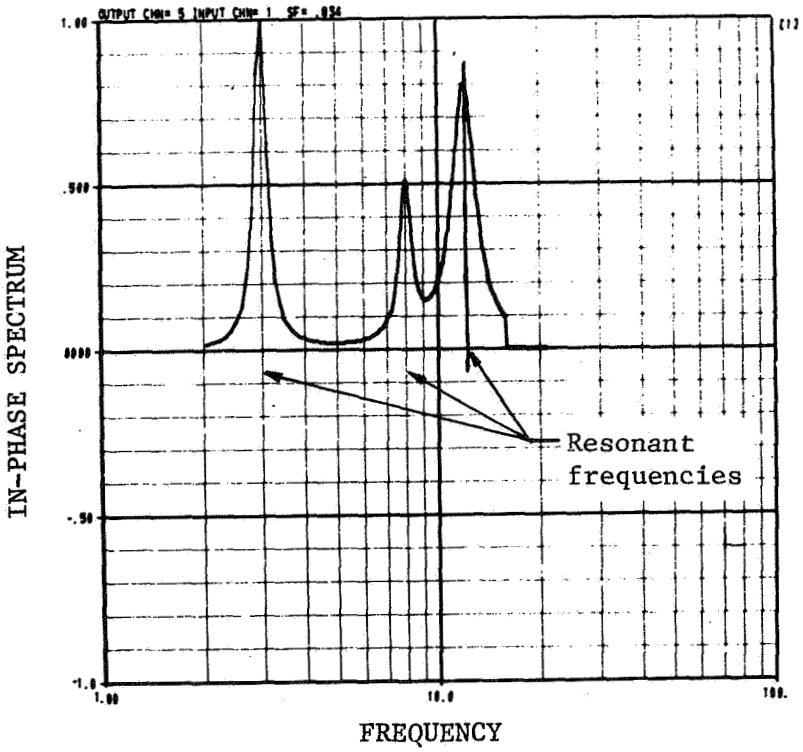

Figure 11. - Annotated in-phase spectrum from COQUAD program.

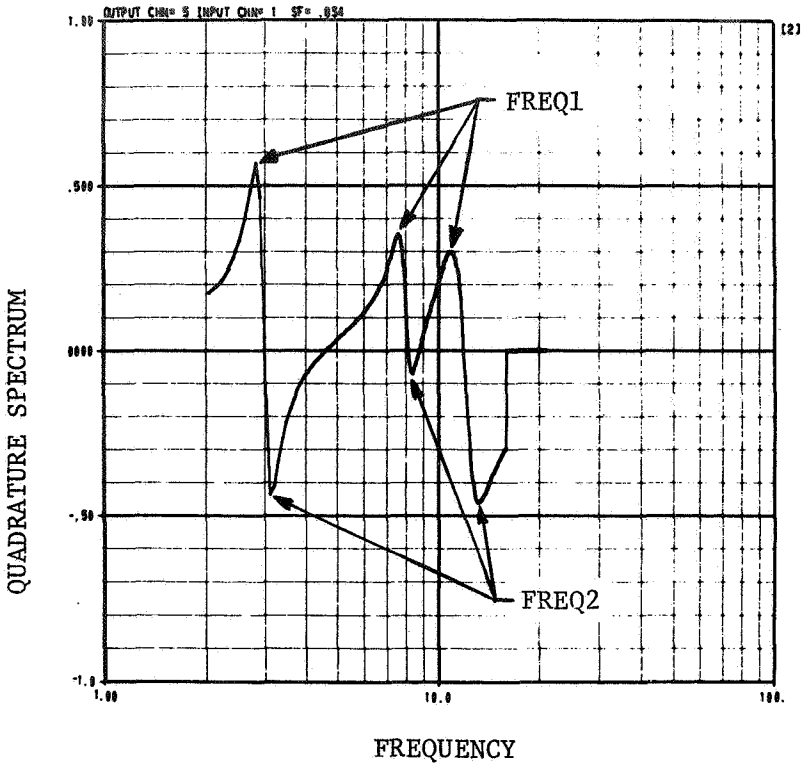

Figure 12. - Annotated quadrature spectrum from COQUAD program.

$$\text{DAMP. COEF.} = \frac{(\text{FREQ2}/\text{FREQ1})^2 - 1}{(\text{FREQ2}/\text{FREQ1})^2 + 1}$$

[3]

XDUCER-CHNL	RES. FREQ.	DAMPING COEF.	FREQ1	FREQ2 [4]
05	3.027	.098	2.852	3.125
05	8.007	.097	7.617	8.398
05	12.01	.104	10.93	13.18

Figure 13. - Annotated output tabulation from COQUAD program.

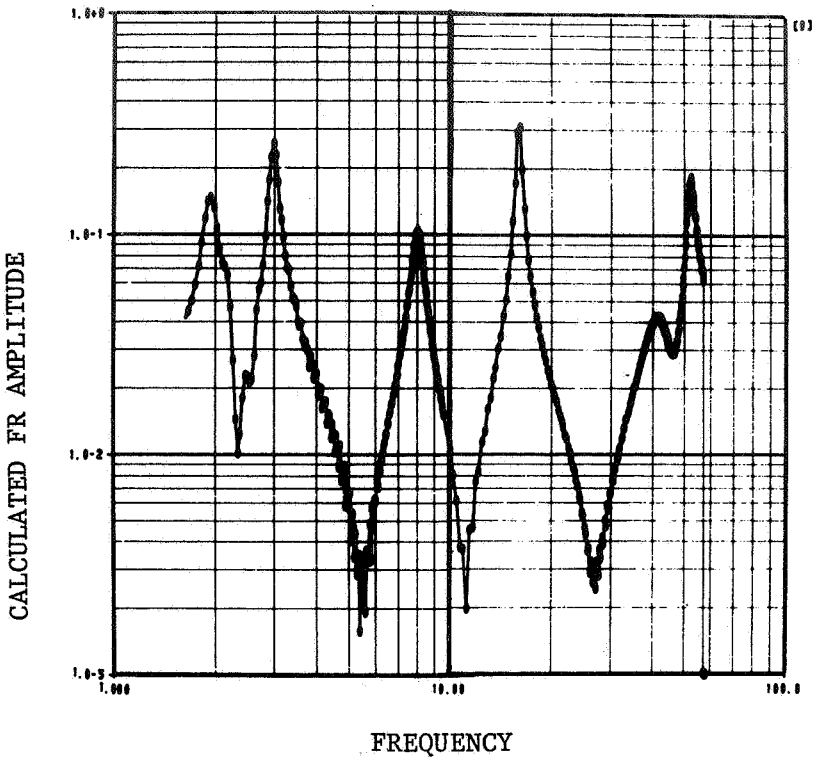

Figure 14. - Calculated frequency response function amplitude from ENERGY program.

ANALYSIS PASS	OUTPUT CHANNEL	RESONANT FREQUENCY	DAMPING COEFFICIENT	MODAL ENERGY	WINDOWING LEVEL	DEGREES OF FREEDOM	XFORM FREQ INCREMENT	ACTUAL FREQ LOWER	WINDOW UPPER
01	09	16.02	.0304	1.657+0	.020	01	.2441	13.2	20.5
01	09	52.11	.0525	4.319-1	.020	02	.2441	35.1	57.0
02	09	16.00	.0202	1.579+0	.010	02	.2441	12.4	22.9
02	09	52.04	.0490	4.357-1	.010	03	.2441	31.7	57.0
01	09	1.970	.1043	2.681-1	.020	01	.0406	1.58	2.21
01	09	3.001	.0501	9.585-1	.020	03	.0406	2.25	4.68
01	09	7.998	.0740	1.388-1	.020	01	.0406	6.64	9.66
02	09	1.999	.0975	2.995-1	.010	03	.0406	1.58	5.56
02	09	3.001	.0498	9.915-1	.010	03	.0406	1.58	5.56
02	09	7.998	.0752	1.476-1	.010	02	.0406	6.30	10.0

Figure 15. - Primary output tabulation from ENERGY program.

ANALYSIS PASS	OUTPUT CHANNEL	RESONANT FREQUENCY	DAMPING COEFFICIENT	MODAL ENERGY	WINDOWING LEVEL	DEGREES OF FREEDOM	POINTS LOADED	ACTUAL FREQ WINDOW LOWER	UPPER
01	09	16.02	.0304	1.657+0	.020	01	00155	13.2	20.5
01	09	43.15	.1920	1.791-2	.020	02	00107	35.1	57.0
01	09	52.11	.0525	4.519-1	020	02	00107	35.1	57.0
02	09	17.56	.1414	2.741-4	.010	02	00154	12.4	22.9
02	09	16.00	.0282	1.579+0	.010	02	00154	12.4	22.9
02	09	41.74	.2027	1.765-2	.010	03	00105	31.7	57.0
02	09	52.04	.0490	4.357-1	.010	03	00105	31.7	57.0
02	09	-.047	-1.00	00000	.010	03	00105	31.7	57.0
02	09	.0029	-1.00	00000	.010	03	00105	31.7	57.0
01	09	1.970	.1043	2.681-1	.020	01	00113	1.58	2.21
01	09	3.001	.0581	9.585-1	.020	03	00273	2.25	4.60
01	09	2.153	.1606	3.354-2	.020	03	00273	2.25	4.60
01	09	5.056	.4000	1.255-3	.020	03	00273	2.25	4.60
01	09	7.990	.0740	1.388-1	.020	01	00105	6.64	9.66
02	09	8.215	.7963	1.052-2	.010	03	00254	1.58	5.56
02	09	1.999	.0975	2.995-1	.010	03	00254	1.58	5.56
02	09	3.001	.0498	9.915-1	.010	03	00254	1.58	5.56
02	09	7.990	.0752	1.476-1	.010	02	00098	6.30	10.0
02	09	.0446	-1.00	00000	.010	02	00098	6.30	10.0

Diagnostic for real difference equation root.

Figure 16. - Annotated secondary output tabulation from ENERGY program.

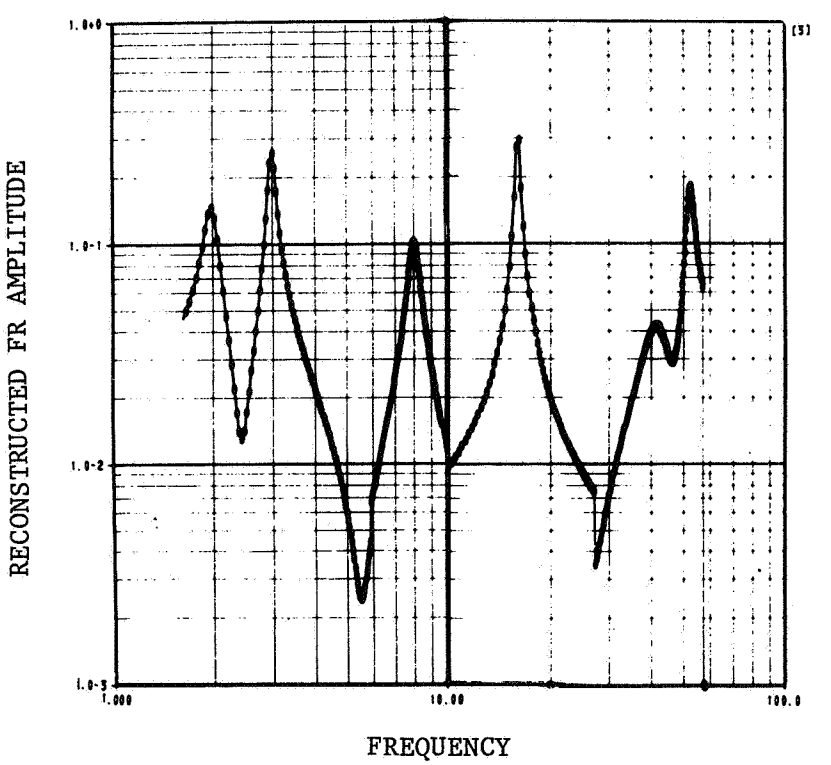

Figure 17. - Reconstructed frequency response function amplitude from ENERGY program.

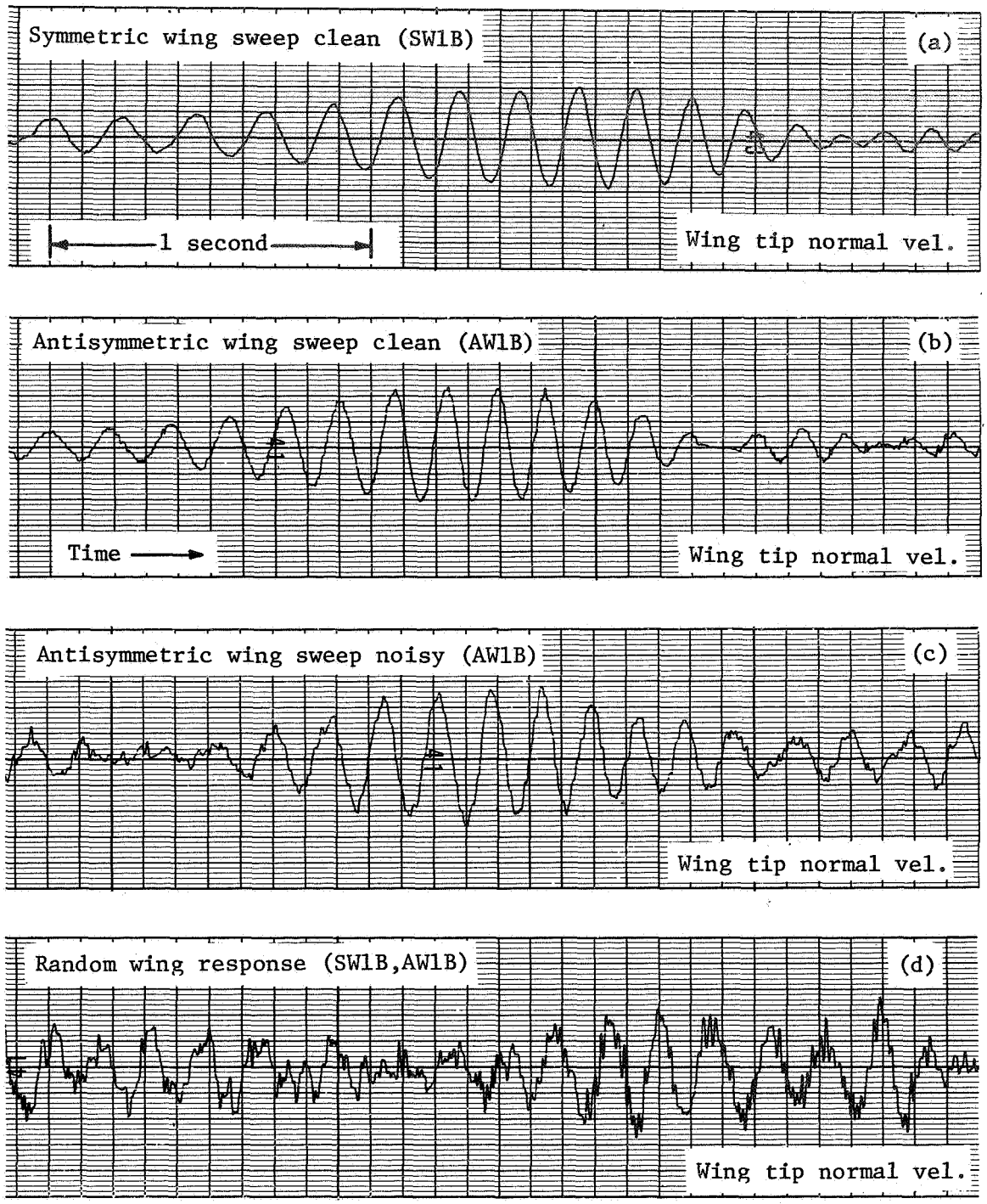

Figure 18.- Flight test flutter response data.

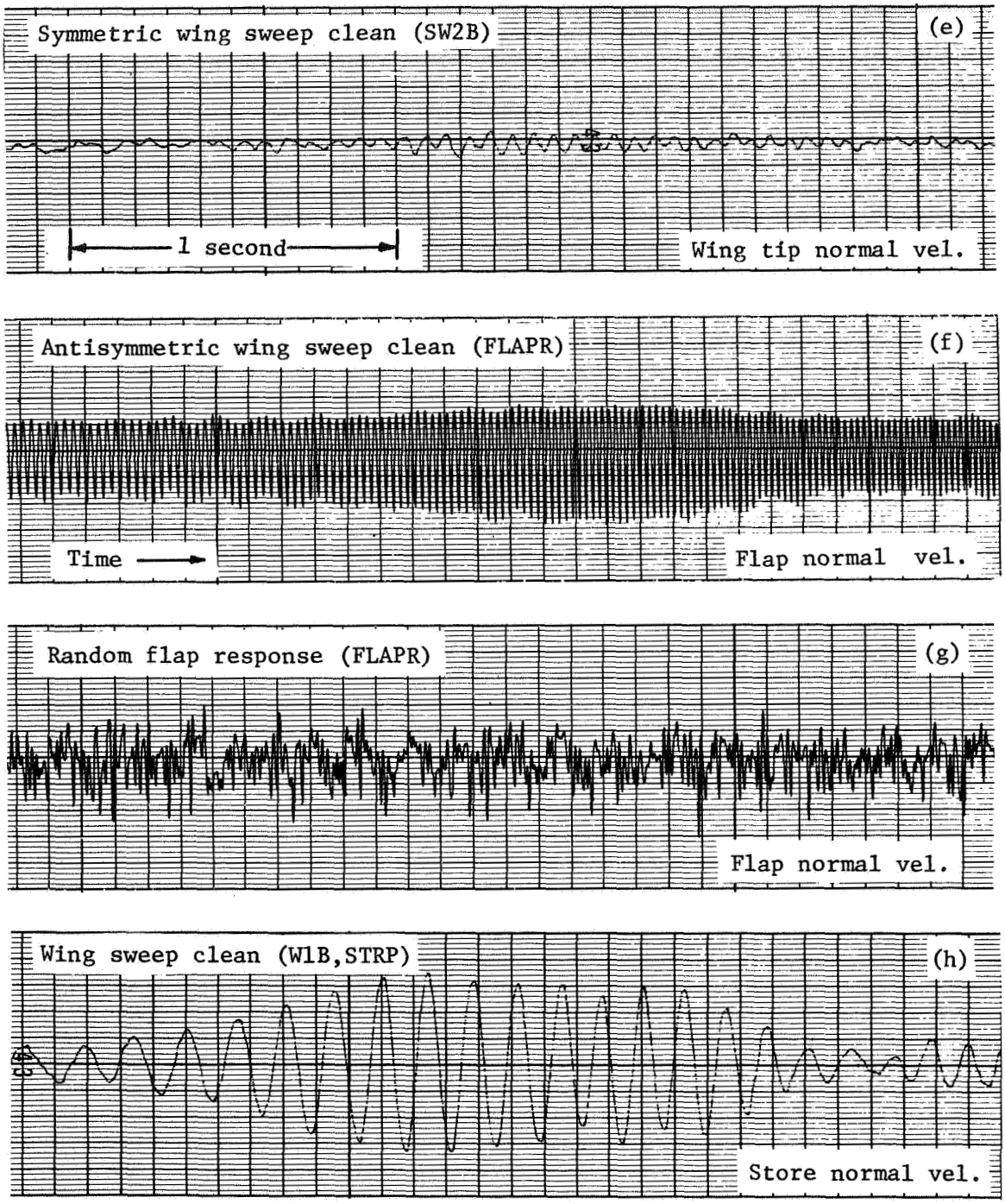

Figure 18. - Concluded.

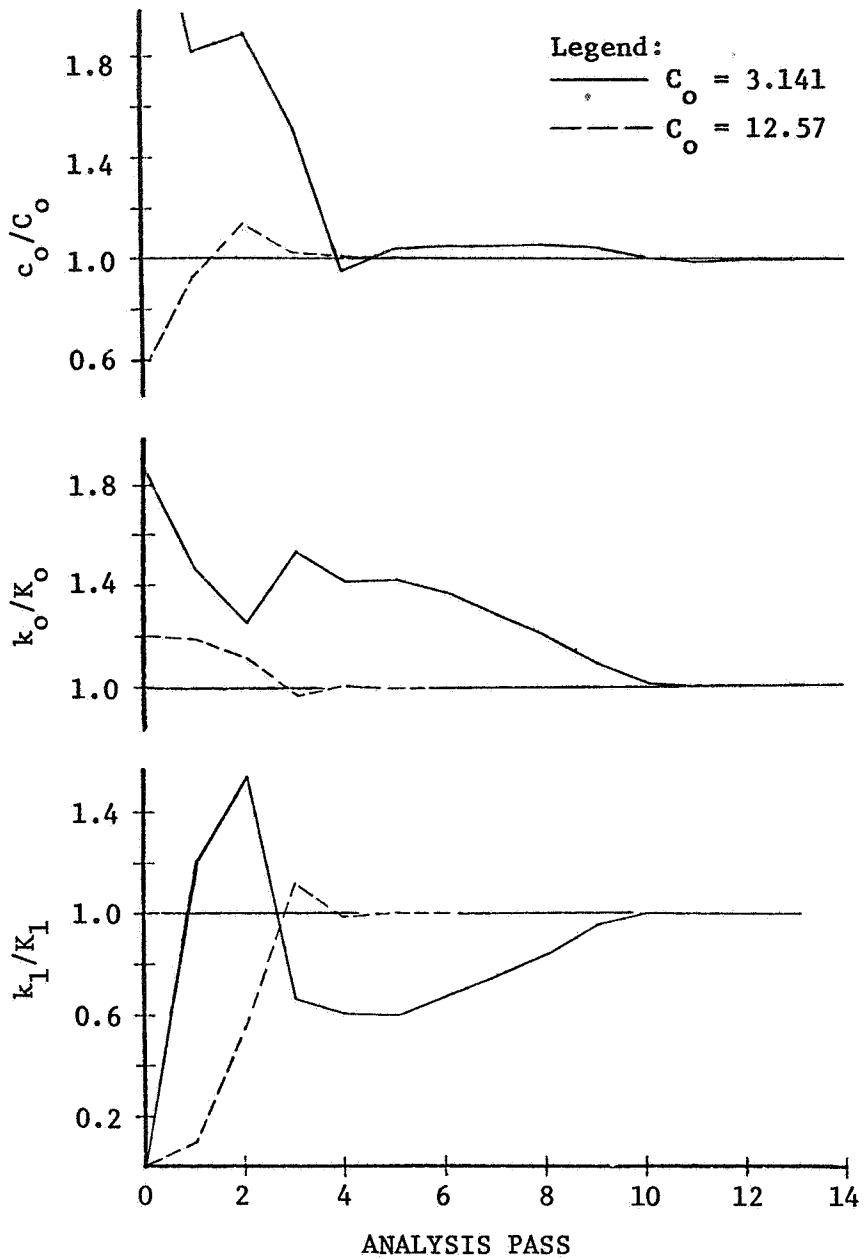

Figure 19. - Parameter convergence for nonlinear model.